

# ACCURATE SOLUTION AND GRADIENT COMPUTATION FOR ELLIPTIC INTERFACE PROBLEMS WITH VARIABLE COEFFICIENTS\*

ZHILIN LI<sup>†</sup>, HAIFENG JI<sup>‡</sup>, AND XIAOHONG CHEN<sup>§</sup>

**Abstract.** A new augmented method is proposed for elliptic interface problems with a piecewise variable coefficient that has a finite jump across a smooth interface. The main motivation is to get not only a second order accurate solution but also a second order accurate gradient *from each side of the interface*. Key to the new method is introducing the jump in the normal derivative of the solution as an augmented variable and rewriting the interface problem as a new PDE that consists of a leading Laplacian operator plus lower order derivative terms near the interface. In this way, the leading second order derivative jump relations are independent of the jump in the coefficient that appears only in the lower order terms after the scaling. An upwind type discretization is used for the finite difference discretization at the irregular grid points on or near the interface so that the resulting coefficient matrix is an M-matrix. A multigrid solver is used to solve the linear system of equations, and the GMRES iterative method is used to solve the augmented variable. Second order convergence for the solution and the gradient from each side of the interface is proved in this paper. Numerical examples for general elliptic interface problems confirm the theoretical analysis and efficiency of the new method.

**Key words.** elliptic interface problem, accurate gradient computation, variable coefficient with discontinuity, interface, M-matrix, convergence proof, discrete Green function

**AMS subject classifications.** 65M06, 65M85, 76M20

**DOI.** 10.1137/15M1040244

**1. Introduction.** In this paper, we develop an efficient numerical method to solve an elliptic interface problem

$$(1.1) \quad \nabla \cdot (\beta(\mathbf{x}) \nabla u(\mathbf{x})) = f(\mathbf{x}), \quad \mathbf{x} \in \Omega \setminus \Gamma, \quad \Omega = \Omega^+ \cup \Omega^-,$$

$$(1.2) \quad [u](\mathbf{X}) = w(\mathbf{X}), \quad [\beta u_n](\mathbf{X}) = v(\mathbf{X}), \quad \mathbf{X} \in \Gamma,$$

in one and two space dimensions, where, for example,  $[u] = [u]_{\Gamma}(\mathbf{X}) = u^+(\mathbf{X}) - u^-(\mathbf{X})$  is the difference of the limiting values of  $u(\mathbf{X})$  from  $\Omega^+$  and  $\Omega^-$  sides, respectively,  $u_n = \mathbf{n} \cdot \nabla u = \frac{\partial u}{\partial n}$  is the normal derivative of solution  $u(\mathbf{X})$ , and  $\mathbf{n}(\mathbf{X})$  is the unit normal direction at a point  $\mathbf{X}$  on the interface pointing to the  $\Omega^+$  side; see Figure 1 for an illustration. The domain and the interface are used in Examples 6.2 and 6.3 in section 6. We use  $\mathbf{x}$  to represent a point in the domain, while  $\mathbf{X}$  is a point on the interface  $\Gamma$ . Since a finite difference discretization will be used, we assume that

\*Received by the editors September 17, 2015; accepted for publication (in revised form) October 24, 2016; published electronically March 15, 2017.

<http://www.siam.org/journals/sinum/55-2/M104024.html>

**Funding:** The first and third authors are partially supported by NSF grant DMS-1522768, NIH grant 5R01GM96195-2, CNSF grants 11371199 and 11471166, and provincial grant BK201411443. The second author is partially supported by grant BK20160880 from the Natural Science Foundation of Jiangsu Province, China.

<sup>†</sup>Center for Research in Scientific Computation and Department of Mathematics, North Carolina State University, Raleigh, NC 27695 (zhilin@math.ncsu.edu).

<sup>‡</sup>School of Science, Nanjing University of Posts and Telecommunications, Jiangsu, Nanjing 210023, China, and Jiangsu Key Laboratory for NSLSCS, Jiangsu, Nanjing 210023, China (hfji@njupt.edu.cn).

<sup>§</sup>Department of Mathematics, North Carolina State University, Raleigh, NC 27695 (xchen30@ncsu.edu).

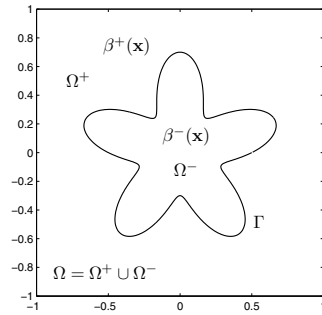


FIG. 1. A diagram of a rectangular domain  $\Omega = \Omega^+ \cup \Omega^-$  with an interface  $\Gamma$ . The coefficient  $\beta(\mathbf{x})$  has a finite jump across the interface  $\Gamma$ . The interface and domain in this figure are used in Examples 6.2 and 6.3 in section 6.

$f(\mathbf{x}) \in C(\Omega^\pm)$ ,  $\beta(\mathbf{x}) \in C^1(\Omega^\pm)$ , excluding  $\Gamma$ , and that  $\Gamma \in C^2$ ,  $w \in C^2(\Gamma)$ ,  $v \in C^1(\Gamma)$ . All the parameters and  $\frac{\partial \beta}{\partial x}$  and  $\frac{\partial \beta}{\partial y}$  are assumed to be bounded. For the regularity requirement of the problem, we also assume that  $\beta(\mathbf{x}) \geq \beta_0 > 0$  and  $f(\mathbf{x}) \in C^\nu(\Omega \setminus \Gamma)$  for a constant  $\nu > 0$  so that  $u(\mathbf{x}) \in C^{2+\nu}(\Omega^\pm)$ ; see [19, 8]. For the error analysis, piecewise higher regularity assumptions are needed for the solution; see sections 3 and 5.

Many free boundary and moving interface problems can be modeled by differential equations involving not only the solution to the governing equations but also the gradient of the solution at the free boundary or the moving interface from each side. Such examples include the Stefan problems and crystal growth modeling the interface between ice and water, in which the velocity of the interface depends on the temperature of the heat equation and its gradient at the interface (called the Stefan condition) [12, 45]; the Hele-Shaw flow [30, 32]; the coupling between a Darcy's system and Stokes or Navier-Stokes equations [36]; and open and traction problems [46, 50]. The most expensive part of simulations from our research on those problems is solving one or more elliptic interface problems, for example, two generalized Helmholtz equations and one Poisson equation when we solve the two-dimensional (2D) incompressible Navier-Stokes equations involving interface using the projection method [46]. The goal of this paper is to present an efficient new finite difference method based on a uniform Cartesian mesh that not only provides an accurate solution globally but also an *accurate gradient* from each side of the interface.

For the elliptic interface problem (1.1)–(1.2), the solution has low global regularity; lower than  $H^1$  is  $w \neq 0$ . Thus, a direct finite difference or finite element method will not work, or will work poorly. Nevertheless, it is reasonable to assume that the solution is piecewise smooth excluding the interface. For example, if the coefficient is a piecewise constant in each subdomain, then the solution in each subdomain is an analytic function in the interior but has a jump in the solution and/or the normal derivative due to the source or dipole distribution from the PDE limiting theory [33]. The gradient used in this paper is defined as the *liming gradient* from each side of the interface.

Naturally, finite element methods can be, and have been, applied to solve the interface problem. It is well known that a second order accurate approximation to the solution of an interface problem with  $w \equiv 0$  and  $v \equiv 0$  can be generated by the Galerkin finite element method with the standard linear basis functions if the triangulation is aligned with the interface; that is, a body fitted mesh is used (see,

for example, [7, 9, 13, 66]). Some kind of posterior techniques or at least quadratic elements is needed in order to get a second order accurate gradient from each side of the interface. The cost in the mesh generation coupled with an unstructured linear solver is hardly competitive with the algorithm proposed in this paper (in our opinion).

There are also quite a few finite element methods using Cartesian meshes. The immersed finite element method (IFEM) was developed for one-dimensional (1D) and 2D interface problems in [40] and [44], respectively. Since then, many IFEMs and analyses have appeared in the literature (see, for example, [14, 25]), with applications shown in [48, 67]. The IFEM is distinguished from other finite element methods (FEMs) in terms of degree of freedom and structure of the coefficient matrix, for example, the extended finite element method (XFEM), in which enrichment functions are added near the interface [60], and the unfitted FEM based on Nitsche's method in [23]. Other related work in this direction can be found in [10, 35, 20, 28] and others. Note that the methods developed in [29, 31] using a Petrov–Galerkin finite element discretization in which the nonconforming immersed finite element (IFE) space and the standard linear finite element space are used as the trial and test functional spaces, respectively. A partial penalty IFE method was proposed in [49]. Other types of method are based on a discontinuous Galerkin [65, 53] or a weak Galerkin [62] method with some penalties. In those methods, some parameters are chosen to achieve the optimal convergence. In general, discontinuous or weak Galerkin methods are flexible because there are more choices of the degree of freedom, which in turn implies these types of methods may be computationally more expensive. These methods are usually better suited for hyperbolic problems and conservation laws. Another interesting development is the spectral solution representation technique [4, 5, 6, 3, 34], which is also based on integral forms. In this technique, the interface problem is decomposed into two problems, one with zero interface data and the other with zero exterior boundary data which is solved by introducing an interface space  $H_\Gamma(\Omega)$  and constructing an orthogonal basis of this space.

Finite difference methods have also played a very important role in scientific computing and in solving engineering problems. Advantages of finite difference methods based on Cartesian meshes include simplicity, ease of programming, and their ability to utilize many existing fast solvers. Note that error estimates from FEMs are based on integral forms, which may not exactly predict the actual errors near the interface compared with estimates from finite difference methods that are based on the pointwise ( $L^\infty$ ) norm. Many new finite difference methods based on Cartesian meshes have been developed for interface problems; see, for example, the ghost fluid method [51], the matched boundary interface method [70], the kernel free boundary integral method [68], and the virtual node method [27]. The difference potential method [16, 59] was developed for 1D elliptic and parabolic problems in [1]. In [54], the difference potential method with second order accuracy in the solution and in the gradient was developed for elliptic interface problems with variable coefficients in [15]. The fourth order extension of the method for the elliptic interface problems was developed in [2].

Most numerical methods for interface problems based on structure meshes are between first and second order accurate for the solution, but the accuracy for the gradient is usually one order lower. Note that the gradient recovering techniques, for example, in [61, 69], usually do not work well for structured meshes because of the arbitrariness of the interface and the underlying mesh. The mixed finite element approach and a few other methods that can find an accurate solution and the gradient simultaneously in the entire domain often lead to a saddle problem and are compu-

tationally expensive; these methods are not ideal choices if we are only interested in the accurate gradient near the interface or boundary. The purpose of this paper is to develop a new method that has a second order accurate solution globally and a second order accurate gradient at the interface. Note that for Poisson equations with singular source along an interface, it was proved in [8] that both the computed solution and the gradient are second order accurate by a factor of  $\log h$  in the infinity norm. In [39], an augmented immersed interface method (AIIM) is proposed to solve the elliptic interface problems with piecewise constant coefficient. Both the solution and the gradient are shown to be second order accurate for all the examples, which will be proved in this paper. The method in [39] provided a clue to accurate gradient computation at the interfaces or boundaries. The method implicitly put the gradient near the interface as an unknown (augmented variable). While there are quite a few accurate and consistent numerical methods for interface problems, the stability of those methods is nevertheless often ignored. In [42], a maximum principle preserving scheme is proposed for variable discontinuous coefficients. A quadratic optimization is used to determine the finite difference coefficients at grid points near the interface so that the coefficient matrix is an M-matrix, which is key to the proof of the convergence of the method. This is another aspect of our method that ensures the coefficient matrix is an M-matrix.

In this paper, we propose a new approach that can provide a second order solution globally and a second order accurate gradient *only* along the interface for a variable coefficient that has a finite jump along the interface. The method has advantages of both of the methods in [39] and [42]. The idea is to introduce the jump in the normal derivative of the solution as an augmented variable. With the augmented variable, the immersed interface method (IIM) is second order accurate both for the solution and first order derivatives [8, 58]. By a suitable transform of the PDE, the leading terms of the second order derivative jump relations needed for the IIM are independent of the coefficient. The lower order derivative terms at irregular grid points that are on or near the interface are discretized using an upwinding discretization within the centered five-point stencil. Thus, the coefficient matrix of the finite difference equations is an M-matrix without using an optimization procedure in [42]. It has been shown that the finite difference solution is second order accurate if the augmented variable is also second order accurate. The augmented variable should be chosen so that the flux jump condition is satisfied. This leads to a second discretization involving the finite difference solution and the augmented variable. The GMRES iteration is utilized to solve the Schur complement for the augmented variable with a new preconditioning strategy. By using the estimates of the discrete Green function, we have shown that the augmented variable has second order accuracy and thus is the finite difference solution.

The rest of the paper is organized as follows. In the next section, we explain the algorithm in one dimension since it is easy to understand, and we follow this with the convergence proof. In section 4, we explain the algorithm in two dimensions followed again by the convergence analysis in section 5. In section 6, we present some 2D numerical examples. We conclude in the last section.

**2. The 1D algorithm.** A model interface problem in one dimension has the form

$$(2.1) \quad \begin{aligned} (\beta u_x)_x &= f(x), & x &\in (a, \alpha) \cup (\alpha, b), \\ u(a) &= u_a, & u(b) &= u_b, & [u]_\alpha &= w, & [\beta u_x]_\alpha &= v, \end{aligned}$$

where  $a < \alpha < b$  is an interface (a point). We assume that conditions for  $\beta(x)$ ,  $f(x)$  described in the introduction hold with  $\Omega^- = (a, \alpha)$  and  $\Omega^+ = (\alpha, b)$ . We will drop the subscript  $\alpha$  in the jump expressions  $[u]_\alpha$  and  $[\beta u_x]_\alpha$  and simply use  $[u]$  and  $[\beta u_x]$  if there is no confusion.

Let  $x_i = a + ih$  be a uniform mesh with  $h = (b - a)/N$  and  $i = 0, 1, \dots, N$ . We define  $q = [u_x]_\alpha$  as the augmented variable. Assume that  $x_j \leq \alpha < x_{j+1}$ . We call  $x_j$  and  $x_{j+1}$  *irregular* grid points, while others are called *regular* grid points. The finite difference scheme at a regular grid point  $x_i$ , with  $i \neq j$  and  $i \neq j + 1$ , can be written as

$$(2.2) \quad \frac{\beta_{i-1/2} U_{i-1} - 2\bar{\beta}_i U_i + \beta_{i+1/2} U_{i+1}}{\beta_i h^2} = \frac{f(x_i)}{\beta_i},$$

where

$$(2.3) \quad \beta_{i-1/2} = \beta(x_i - h/2), \quad \beta_{i+1/2} = \beta(x_i + h/2), \quad \bar{\beta}_i = \frac{\beta_{i-1/2} + \beta_{i+1/2}}{2}.$$

At the irregular grid points  $x_j$  and  $x_{j+1}$ , we use the equivalent differential equation

$$(2.4) \quad u_{xx} + \frac{\beta_x u_x}{\beta} = \frac{f}{\beta}.$$

This is one of the key ideas of the new augmented approach. In this way, we can get second order derivative jump conditions  $[u_{xx}]$  in terms of lower order derivative jump conditions and derivatives of the solution.

If we know the jump  $[u_x] = q$  in addition to the original jump conditions  $[u]$  and  $[\beta u_x]$ , then we know the jump relations

$$(2.5) \quad \begin{aligned} [u] &= w, & [u_x] &= q, \\ [u_{xx}] &= \left[ \frac{f}{\beta} \right] - \frac{\beta_x^+ u_x^+}{\beta^+} + \frac{\beta_x^- u_x^-}{\beta^-} = \left[ \frac{f}{\beta} \right] - \left[ \frac{\beta_x}{\beta} \right] u_x^- - \frac{\beta_x^+}{\beta^+} q. \end{aligned}$$

If  $\beta_x(x_j)/\beta(x_j) \geq 0$ , then the finite difference discretization at the irregular grid point  $x_j$  can be written as

$$(2.6) \quad \frac{U_{j-1} - 2U_j + U_{j+1}}{h^2} + C^{FD}(U_{j-1}, U_j, U_{j+1}) + \frac{\beta_x(x_j)}{\beta(x_j)} \left( \frac{U_{j+1} - U_j}{h} + C \right) = \frac{f(x_j)}{\beta(x_j)},$$

where  $C$  is a correction term (see [43]),

$$(2.7) \quad C = -\frac{[u]}{h} - \frac{(x_{j+1} - \alpha)[u_x]}{h} = -\frac{w}{h} - \frac{(x_{j+1} - \alpha)q}{h},$$

and  $C^{FD}(U_{j-1}, U_j, U_{j+1})$  is part of the finite difference equation,

$$(2.8) \quad \begin{aligned} C^{FD}(U_{j-1}, U_j, U_{j+1}) &= -\frac{[u]}{h^2} - \frac{(x_{j+1} - \alpha)[u_x]}{h^2} - \frac{(x_{j+1} - \alpha)^2[u_{xx}]}{2h^2} \\ &= -\frac{w}{h^2} - \frac{(x_{j+1} - \alpha)q}{h^2} - \frac{(x_{j+1} - \alpha)^2[u_{xx}]}{2h^2}, \end{aligned}$$

in which  $[u_{xx}]$  is discretized by (see (2.5))

$$[u_{xx}] = \left[ \frac{f}{\beta} \right] - \left[ \frac{\beta_x}{\beta} \right] u_x - \frac{\beta_x^+}{\beta^+} q$$

$$\approx \begin{cases} \left[ \frac{f}{\beta} \right] - \frac{\beta_x^+}{\beta^+} q - \left[ \frac{\beta_x}{\beta} \right] \frac{U_j - U_{j-1}}{h} & \text{if } \left[ \frac{\beta_x}{\beta} \right] \leq 0, \\ \left[ \frac{f}{\beta} \right] - \frac{\beta_x^+}{\beta^+} q - \left[ \frac{\beta_x}{\beta} \right] \left( \frac{U_{j+1} - U_j}{h} + C \right) & \text{otherwise.} \end{cases}$$

The case when  $\beta_x(x_j)/\beta(x_j) < 0$  can be treated in a similar way. We omit the details. We can derive a similar finite difference scheme at the irregular grid point  $x_{j+1}$ . The finite difference scheme has the following properties:

- It is consistent. The local truncation errors at regular grid points are  $O(h^2)$ , and they are  $O(h)$  at irregular grids points  $x_j$  and  $x_{j+1}$ .
- The finite difference scheme can be written as

$$(2.9) \quad A_h \mathbf{U} + BQ = \mathbf{F}_1,$$

where the coefficient matrix  $A_h$  is an M-matrix, irreducible, tridiagonal, and diagonally dominant,  $\mathbf{U}$  is the column vector formed by the finite difference solution,  $B$  is a column vector with at most two nonzero entries at  $j$ th and  $(j+1)$ th locations, and  $Q$  is the approximate value of  $q = [u_x]$ . Note that  $A_h$  is invertible and that the two components of  $F_j$  and  $F_{j+1}$  have been modified.

**2.1. Discretization of the flux jump condition.** Next we discuss the interpolation scheme to approximate the interface condition  $[\beta u_x] = v$ . First, we rewrite the jump condition as

$$(2.10) \quad [\beta u_x] = \beta^+ u_x^+ - \beta^- u_x^- = \beta^+ (u_x^- + q) - \beta^- u_x^-$$

$$\implies \frac{\beta^+ - \beta^-}{\beta^+} u_x^- + q = \frac{v}{\beta^+}.$$

This can be discretized as

$$(2.11) \quad \frac{\beta^+ - \beta^-}{\beta^+} (\gamma_1 U_{j-1} + \gamma_2 U_j + \gamma_3 U_{j+1} + C_3) + q = \frac{v}{\beta^+},$$

where  $\gamma_1, \gamma_2, \gamma_3$ , and the correction term  $C_3$  are determined using the idea of the IIM so that the interpolation scheme is a second order approximation of (2.10), that is,

$$\frac{\beta^+ - \beta^-}{\beta^+} (\gamma_1 u(x_{j-1}) + \gamma_2 u(x_j) + \gamma_3 u(x_{j+1}) + C_3) + [u_x] - \frac{v}{\beta^+} = O(h^2).$$

In the matrix-vector form, the above equation can be written as

$$(2.12) \quad S\mathbf{U} + GQ = F_2,$$

where  $S$  is a row vector whose sum is zero.

We define the residual of the flux jump condition given an approximation  $Q$  as

$$(2.13) \quad R(Q) = S\mathbf{U} + GQ - F_2,$$

which is the discrete form of  $r(q) = [\beta u_x] - v$ . If we put (2.9) and (2.12) together, we get

$$(2.14) \quad \begin{bmatrix} A_h & B \\ S & G \end{bmatrix} \begin{bmatrix} \mathbf{U} \\ Q \end{bmatrix} = \begin{bmatrix} \mathbf{F}_1 \\ F_2 \end{bmatrix}.$$

Eliminating  $\mathbf{U}$  in (2.14) gives the Schur complement equation for  $Q$ ,

$$(2.15) \quad (G - SA_h^{-1}B)Q = F_2 - SA_h^{-1}\mathbf{F}_1.$$

Equation (2.15) can be solved if the Schur complement is nonsingular. Once  $Q$  is computed, one can substitute it in (2.9) to solve for  $\mathbf{U}$ . The cost of computation in this process is solving linear systems with the form  $A_h x = b$  three times,  $A_h^{-1}\mathbf{F}_1$ ,  $A_h^{-1}BQ$ , and finally (2.9). Since matrix  $A_h$  is tridiagonal and row diagonally dominant, the Thomas algorithm is guaranteed to be stable, and the solution can be obtained in  $O(N)$  operations.

**3. Convergence analysis of the 1D algorithm.** In this section, we show second order convergence of the solution globally, its first order derivative at the interface, and the augmented variable of the proposed new method. The proof is simpler than that of the 2D case but serves the purpose of understanding the tools used in the proof of the 2D case in section 5.

We use the following notation. We denote the errors as  $\mathbf{E}^u = \mathbf{U} - \mathbf{u}$  with  $\mathbf{E}_i^u = U_i - u(x_i)$  for the solution and  $E^q = Q - q$  for the augmented variable, respectively, where  $u(x_i)$  is the true solution at  $x_i$ . We use  $C$  to represent a generic error constant. We start the analysis by assuming that the coefficient  $\beta(x)$  is a piecewise constant, the domain is  $(0, 1)$ , and a Dirichlet boundary condition is prescribed at the two end points for simplicity.

**THEOREM 3.1.** *Assume that  $\beta(x)$  is a piecewise constant and  $u(x)$  is in piecewise  $C^4$  excluding the interface  $\alpha$ . If  $Q$  is a second order accurate approximation to  $q$ , i.e.,  $|E^q| \leq Ch^2$ , then we also have  $\|\mathbf{E}^u\|_\infty \leq Ch^2$ .*

*Proof.* Let  $\mathbf{T}^u$  be the local truncation error of system (2.9), that is,

$$(3.1) \quad A_h \mathbf{u} + Bq = \mathbf{F}_1 + \mathbf{T}^u,$$

where  $\mathbf{u}$  is the vector formed by the true solution at the grid points  $x_i$ , and  $q$  is the jump of the derivative of the solution  $[u_x]$  across the interface  $\alpha$ . Subtracting (3.1) from (2.9) yields

$$(3.2) \quad A_h \mathbf{E}^u = \tilde{\mathbf{F}}^u,$$

where  $\tilde{\mathbf{F}}^u = -\mathbf{T}^u - BE^q$ . Notice that  $|\mathbf{T}_i^u| \leq Ch^2$  and  $B_i = 0$  at regular grid points, while  $|\mathbf{T}_j^u| \leq Ch$ ,  $|\mathbf{T}_{j+1}^u| \leq Ch$  and  $B_j \sim O(\frac{1}{h})$ ,  $B_{j+1} \sim O(\frac{1}{h})$ . Since  $|E^q| \leq Ch^2$ , we have  $\tilde{F}_i^u \approx O(h^2)$  at regular points, while  $\tilde{F}_j^u \sim O(h)$ ,  $\tilde{F}_{j+1}^u \sim O(h)$ . Also when  $\beta$  is piecewise constant, the matrix  $A_h$  can be simplified as

$$A_h = \frac{1}{h^2} \begin{bmatrix} -2 & 1 & & \\ 1 & -2 & 1 & \\ \dots & \dots & \dots & \dots \\ & & 1 & -2 \end{bmatrix}.$$

From [37], we have

$$(3.3) \quad (A_h)_{ij}^{-1} = hG(x_i; x_j) = \begin{cases} h(x_j - 1)x_i, & i = 1, 2, \dots, j, \\ h(x_i - 1)x_j, & i = j, j + 1, \dots, N - 1, \end{cases}$$

where

$$G(x; \bar{x}) = \begin{cases} (\bar{x} - 1)x, & x \leq \bar{x}, \\ (x - 1)\bar{x}, & x \geq \bar{x}, \end{cases}$$

is the Green function, that is, the solution of

$$\begin{aligned}\Delta_x G(x; \bar{x}) &= \delta(x - \bar{x}), \quad 0 < x < 1, \quad 0 < \bar{x} < 1, \\ G(0; \bar{x}) &= 0, \quad G(1; \bar{x}) = 0.\end{aligned}$$

The global error of  $u$  then can be represented as

$$(3.4) \quad E_i^u = h \sum_{j=1}^{N-1} \tilde{F}_j^u G(x_i; x_j).$$

Since  $0 \leq G(x_i; x_j) \leq 1$ , we have the inequality

$$\begin{aligned}|E_i^u| &\leq \left| h \sum_{j=1}^{N-1} \tilde{F}_j^u \right| \leq h \left( |\tilde{F}_j^u| + |\tilde{F}_{j+1}^u| + \sum_{k=1}^{j-1} |\tilde{F}_k^u| + \sum_{k=j+2}^{N-1} |\tilde{F}_k^u| \right) \\ &\sim h (O(h) + (N-2)O(h^2)) \sim O(h^2),\end{aligned}$$

since  $N \sim 1/h$ . This shows that  $\|E^u\|_\infty \leq Ch^2$ , and hence the proof is complete.  $\square$

Next we show that the Schur complement system is nonsingular.

**THEOREM 3.2.** *With the same assumptions as in Theorem 3.1 and  $\beta^- \neq \beta^+$ , the coefficient matrix (a number for the 1D problem) of the Schur complement is nonsingular.*

*Proof.* Note that from (2.9), that is,  $A_h \mathbf{U}(Q) + BQ = \mathbf{F}_1$ , we have  $A_h^{-1}BQ = A_h^{-1}\mathbf{F}_1 - \mathbf{U}(Q)$ , and the Schur complement can be rewritten as

$$\begin{aligned}(G - SA_h^{-1}B)Q &= GQ - SA_h^{-1}BQ = GQ - SA_h^{-1}\mathbf{F}_1 + S\mathbf{U}(Q) \\ &= (S\mathbf{U}(Q) + GQ) - (SA_h^{-1}\mathbf{F}_1 + G \cdot 0) \\ &= (S\mathbf{U}(Q) + GQ) - (S\mathbf{U}(0) + G \cdot 0) \\ &= R(Q) - R(0).\end{aligned}$$

If  $Q \neq 0$  and  $\beta^- \neq \beta^+$ , then  $R(Q) \neq R(0)$ . For the 1D problem, we have  $(G - SA_h^{-1}B)1 = (G - SA_h^{-1}B)1 = R(1) - R(0) \neq 0$ .<sup>1</sup>  $\square$

Now we are ready to show that the augmented variable  $Q$  is also second order accurate.

**THEOREM 3.3.** *With the same assumptions as in Theorem 3.1 and  $\beta^- \neq \beta^+$ , we have  $|E^q| = |Q - q| \leq Ch^2$ .*

*Proof.* Similarly to the definition of the local truncation error  $\mathbf{T}^u$ , we define the local truncation  $T^q$  of  $q$  as

$$(3.5) \quad S\mathbf{u} + Gq = F_2 + T^q,$$

where  $\mathbf{u}$  and  $q$  are defined as before. From (2.14), we know that

$$(3.6) \quad \begin{bmatrix} A & B \\ S & G \end{bmatrix} \begin{bmatrix} \mathbf{E}^u \\ E^q \end{bmatrix} = \begin{bmatrix} -\mathbf{T}^u \\ -T^q \end{bmatrix}.$$

<sup>1</sup>Note that some of the proof is similar to section 6.1.2 of [43].



Eliminating  $\mathbf{E}^u$ , we get the Schur complement system for  $E^q$ ,

$$(3.7) \quad (G - SA^{-1}B)E^q = -T^q + SA^{-1}\mathbf{T}^u.$$

We already know that  $(G - SA^{-1}B)$  is nonsingular and  $\|T^q\|_\infty \leq Ch^2$ . The key is to show that  $\|SA^{-1}\mathbf{T}^u\|_\infty \leq Ch^2$ .

Let  $\mathbf{b} = A^{-1}\mathbf{T}^u$ ; from the definition of the Green function in (3.3), we can write

$$(3.8) \quad b_i = h \sum_{l=1}^{N-1} \mathbf{T}_j^u G(x_i; x_l).$$

At first glance, it seems that  $E^q \sim O(h)$  since the interpolation operator  $\|S\|_\infty \sim 1/h$ . Nevertheless, the following analysis shows that  $E^q \sim O(h^2)$  is actually true. Let  $\Delta_i = b_i - b_{i-1}$ ,  $i = 2, \dots, N-1$ . Then we have (note that both  $SA^{-1}\mathbf{T}^u$  and  $S\mathbf{b}$  are scalars for the 1D problem)

$$\begin{aligned} SA^{-1}\mathbf{T}^u &= S\mathbf{b} = S_{j-1}b_{j-1} + S_j b_j + S_{j+1}b_{j+1} \\ &= S_{j-1}(b_j - \Delta_j) + S_j b_j + S_{j+1}(b_j + \Delta_{j+1}) \\ &= (S_{j-1} + S_j + S_{j+1})b_j - S_{j-1}\Delta_j + S_{j+1}\Delta_{j+1} \\ &= -S_{j-1}\Delta_j + S_{j+1}\Delta_{j+1}. \end{aligned}$$

Notice the term  $b_j$  is cancelled out. This is because the interpolation operator is for the first order derivative of  $u(x)$ , and the consistency condition requires that  $S_{j-1} + S_j + S_{j+1} = 0$ . Now what is left to prove is that  $\Delta_j \sim \Delta_{j+1} \sim O(h^3)$ , which leads to  $E^q \sim h^2$ , since  $S_{j-1} \sim S_{j+1} \sim O(1/h)$ . The final step of the proof is explained below.

$$\begin{aligned} |\Delta_i| &= |b_i - b_{i-1}| = h \sum_{l=1}^{N-1} |\mathbf{T}_l^u| \cdot |G(x_i; x_l) - G(x_{i-1}; x_l)| \\ &\leq h^2 \sum_{l \neq j, j+1}^{N-1} |\mathbf{T}_l^u| + h^2 (|T_j^u| + |T_{j+1}^u|) \quad \text{from the continuity of } G(x_i, x_l) \\ &\approx O(h^3). \end{aligned}$$

This completes the proof.  $\square$

As the result of Theorems 3.1–3.3, we conclude that the solution  $\mathbf{U}$  is also second order approximation to  $\mathbf{u}$ , which is summarized in the following theorem.

**THEOREM 3.4.** *With the same assumptions as in Theorem 3.1,  $\beta^- \neq \beta^+$ , and  $\beta$  piecewise constant,  $\|\mathbf{E}^u\|_\infty = \|\mathbf{U} - \mathbf{u}\|_\infty \leq Ch^2$ .*

*Proof.* Since the Schur complement matrix is a constant independent of  $h$ ,  $|T^q| \leq Ch^2$ , and  $|SA^{-1}\mathbf{T}^u| \leq Ch^2$  just proved, from (2.15) we have the conclusion.  $\square$

We get not only a second order accurate solution and the augmented variable, but also second order accurate derivatives  $u_x^-$  and  $u_x^+$  if the derivative is computed using the scheme (2.10), that is,

$$(3.9) \quad u_x^- = \frac{\beta^+}{\beta^+ - \beta^-} \left( \frac{v}{\beta^+} - q \right),$$

assuming that  $\beta^- \neq \beta^+$ . Since the computed  $Q$  is second order accurate, we immediately have the following theorem.

TABLE 1

A grid refinement analysis for the Stefan problem at the final time  $t = 3$ . The computed solution, the first order derivative  $u_x^-(\alpha(t))$ , and the free boundary  $\alpha(t)$  all have average second order convergence.

$N$	$\ u - U\ _\infty$	$r$	$\ u_x - Q\ $	$r$	$ \alpha - \mathcal{A} $	$r$
16	$2.3160 \times 10^{-2}$		$3.9232 \times 10^{-4}$		$4.0734 \times 10^{-2}$	
32	$6.4260 \times 10^{-3}$	1.8496	$3.0046 \times 10^{-4}$	0.3849	$1.1473 \times 10^{-2}$	1.8280
64	$1.9403 \times 10^{-3}$	1.7276	$1.2357 \times 10^{-5}$	4.6038	$3.5210 \times 10^{-3}$	1.7042
128	$4.8957 \times 10^{-4}$	1.9867	$1.8056 \times 10^{-7}$	6.0967	$8.8986 \times 10^{-4}$	1.9843
256	$1.0044 \times 10^{-4}$	2.2852	$7.3479 \times 10^{-8}$	1.2971	$1.7986 \times 10^{-4}$	2.3067

**THEOREM 3.5.** Assume  $\beta$  is two different piecewise constants and  $U_x^-$  is computed using the above formula with  $q$  being replaced by  $Q$ , the computed augmented variable. Then  $|U_x^- - u_x^-| \leq Ch^2$ , where  $u_x^- = \lim_{x \rightarrow \alpha^-} \frac{du}{dx}(x)$ .

**3.1. An example of the 1D Stefan problem.** Our numerical experiments in one dimension have confirmed our theoretical analysis that both the solution  $U \approx u(x)$  and the augmented variable  $Q \approx [u_x]$  are second order accurate in the  $L^\infty$  norm. We show an example of the 1D Stefan problem (see, for example, [11, 18]), in which the free boundary  $\alpha(t)$  is moving. The governing equations are

$$\begin{aligned} \frac{\partial u}{\partial t} &= \frac{\partial^2 u}{\partial x^2} \quad \text{for } 0 < x < \alpha(t), \quad t > 0, \\ u(x, t) &= 0 \quad \text{for } x \geq \alpha(t), \quad t > 0, \end{aligned}$$

where  $\alpha(t)$  is subject to the Stefan condition,

$$\frac{d\alpha}{dt}(t) = -\frac{\partial u}{\partial x}(\alpha(t), t), \quad \alpha(0) = 0.$$

The boundary and initial conditions are

$$\frac{\partial u}{\partial x}(0, t) = f(t), \quad u(\alpha(t), t) = 0, \quad u(x, 0) = 0.$$

The model is from [55]. We use the following exact solution:

$$u(x, t) = 1 - \frac{\operatorname{erf}(x/(2\sqrt{t}))}{\operatorname{erf}(\omega)}, \quad \alpha(t) = 2\omega\sqrt{t},$$

where  $\operatorname{erf}$  is the error function and  $\omega$  is the solution of the transcendental equation  $\sqrt{\pi}\omega \cdot \operatorname{erf}(\omega)e^{\omega^2} = 1$ . The function  $f(t, \alpha(t))$  is determined from the analytic solution.

We use a second order time splitting technique to solve the problem; that is, we solve the differential equation with  $\alpha(t)$  fixed, then update the new location of  $\alpha(t)$ . The augmented equation now is the boundary condition at  $\alpha(t)$ . In Table 1, we show a grid refinement analysis of the errors in the solution at all grid points, the free boundary  $\alpha(t)$ , and the first order derivative  $u_x^-(\alpha(t))$  at the final time  $t = 3$ . We use lowercase letters for the analytic solutions and uppercase letters for the computed solutions. We observe that all of them have average second order convergence.

**4. The algorithm for 2D problems.** In this section, we present the algorithm for 2D problems. The key is the modification of the finite difference scheme at irregular grid points. We first discuss the interface relations using an equivalent representation of the interface problem.

**4.1. The jump relations in the local coordinates.** As explained in the introduction, we rewrite the elliptic interface problem near the interface as

$$(4.1) \quad \Delta u + \frac{\beta_x}{\beta} u_x + \frac{\beta_y}{\beta} u_y = \frac{f}{\beta},$$

$$(4.2) \quad [u]_\Gamma = w, \quad [u_n]_\Gamma = q,$$

where  $q(\mathbf{X})$  is the augmented variable only defined along the interface  $\Gamma$  which should be chosen such that the flux jump condition

$$[\beta u_n]_\Gamma(\mathbf{X}) = v(\mathbf{X})$$

is satisfied. In this way, the Laplacian term  $\Delta u$  has been separated from  $\beta(x, y)$  which makes the discretization easier with our proposed augmented method. This is one of the key ideas of the new method.

From the descriptions in both [38, section 3.1] and [43, section 3.1], we restate some theoretical results on the reformulated elliptic interface problem (4.1)–(4.2). Assume that the interface in the parametric form is

$$(4.3) \quad \Gamma = \left\{ (X(s), Y(s)), \quad X(s) \in C^2, \quad Y(s) \in C^2 \right\},$$

where  $s$  is a parameter, for example, the arc-length. At a point of the interface  $(X, Y)$ , the local coordinate system in the normal and tangential directions is defined as (see Figure 2 for an illustration)

$$(4.4) \quad \begin{cases} \xi = (x - X) \cos \theta + (y - Y) \sin \theta, \\ \eta = -(x - X) \sin \theta + (y - Y) \cos \theta, \end{cases}$$

where  $\theta$  is the angle between the  $x$ -axis and the normal direction, pointing to the  $\Omega^+$  subdomain. Under such a new coordinates system, the interface can be parameterized as

$$(4.5) \quad \xi = \chi(\eta) \quad \text{with} \quad \chi(0) = 0, \quad \chi'(0) = 0.$$

The curvature of the interface at  $(X, Y)$  is  $\chi''(0)$ .

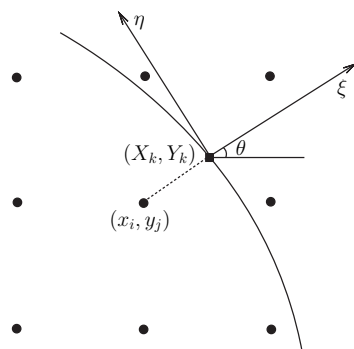


FIG. 2. A diagram of an irregular grid point  $(x_i, y_j)$ , its orthogonal projections on the interface  $(X_k, Y_k)$ , and the local coordinates at  $(X_k, Y_k)$  in the normal and tangential directions.

If we know the jump in the solution  $[u] = w$  and the normal derivative  $[u_n] = q$  (not the original flux jump condition  $[\beta u_n] = v$ ), then we can have the following jump relations at a point  $(X, Y)$  on the interface which is necessary to derive the accurate finite difference method.

**THEOREM 4.1.** *For the elliptic interface problem (4.1)–(4.2), if we are given  $[u] = w$  and  $[u_n] = q$ , then at the interface the following jump relations hold:*

$$(4.6) \quad \begin{aligned} [u] &= w, & [u_\eta] &= w', & [u_\xi] &= q, \\ [u_{\eta\eta}] &= -q\chi'' + w'', & [u_{\xi\eta}] &= w'\chi'' + q', \\ [u_{\xi\xi}] &= q\left(\chi'' - \frac{\beta_\xi^+}{\beta^+}\right) - w'' - \left[\frac{\beta_\xi}{\beta}\right]u_\xi^- - \left[\frac{\beta_\eta}{\beta}\right]u_\eta^- - \frac{\beta_\eta^+}{\beta^+}w' + \left[\frac{f}{\beta}\right], \end{aligned}$$

where  $w'$ ,  $g'$ , and  $w''$  are the first and second order surface derivatives of  $w$  and  $g$  on the interface, and are all evaluated at  $(\xi, \eta) = (0, 0)$ .

Here we skip the derivation, which is similar to those derived in (3.5) in section 3.1 of [43], assuming that  $[u] = w$  and  $[\beta u_n] = v$  are given. Note also that we can express the jump conditions in terms of  $u^+$ ,  $u_\eta^+$ , and  $u_\xi^+$ .

Once we have the jump relations in the local coordinates, we can get back the jump relations in the  $x$ - and  $y$ -directions according to (9.47) in [43] as follows:

$$(4.7) \quad \begin{aligned} [u_x] &= [u_\xi] \cos \theta - [u_\eta] \sin \theta, & [u_y] &= [u_\xi] \sin \theta + [u_\eta] \cos \theta, \\ [u_{xx}] &= [u_{\xi\xi}] \cos^2 \theta - 2[u_{\xi\eta}] \cos \theta \sin \theta + [u_{\eta\eta}] \sin^2 \theta, \\ [u_{yy}] &= [u_{\xi\xi}] \sin^2 \theta + 2[u_{\xi\eta}] \cos \theta \sin \theta + [u_{\eta\eta}] \cos^2 \theta. \end{aligned}$$

**4.2. The finite difference scheme for the 2D problem.** For simplification, we use a uniform mesh

$$(4.8) \quad x_i = a + ih, \quad i = 0, 1, \dots, M; \quad y_j = c + jh, \quad j = 0, 1, \dots, N,$$

assuming  $\Omega = (a, b) \times (c, d)$ . The interface  $\Gamma$  is represented by the zero level set of a Lipschitz continuous function  $\varphi(x, y)$ , that is,

$$(4.9) \quad \Gamma = \left\{ (x, y), \quad \varphi(x, y) = 0, \quad (x, y) \in \Omega \right\}.$$

In the neighborhood of the interface, we assume that  $\varphi(x, y) \in C^2$ . In implementation, the level set function is defined at the grid points as  $\{\varphi_{ij}\}$  corresponding to  $\varphi(x_i, y_j)$ . At a grid point  $(x_i, y_j)$ , we define

$$(4.10) \quad \varphi_{ij}^{max} = \max \{ \varphi_{i-1,j}, \varphi_{ij}, \varphi_{i+1,j}, \varphi_{i,j-1}, \varphi_{i,j+1} \},$$

$$(4.11) \quad \varphi_{ij}^{min} = \min \{ \varphi_{i-1,j}, \varphi_{ij}, \varphi_{i+1,j}, \varphi_{i,j-1}, \varphi_{i,j+1} \}.$$

A grid point  $(x_i, y_j)$  is called *regular* if  $\varphi_{ij}^{max} \varphi_{ij}^{min} > 0$ ; otherwise it is called *irregular*.

The set of orthogonal projections  $(X_k, Y_k)$ ,  $k = 1, 2, \dots, N_b$ , of all irregular grid points on the interface from a particular side, say  $\Omega^+$ , forms a discretization of the interface  $\Gamma$ . We refer the reader to section 1.6.4 in [43] on how to find approximate orthogonal projections. Then the discrete augmented variable  $Q_k$  of the continuous  $q(s)$  is defined at those orthogonal projections. Given a discrete quantity along the interface, we can interpolate the quantity at the discrete points to get its value and

the tangential derivative anywhere along the interface. For example, assume that  $(x_i, y_j)$  is an irregular grid point, and the interface cuts the grid line at  $(x_{ij}^*, y_j)$  corresponding to the orthogonal projection  $\mathbf{X}_k = (X_k, Y_k)$ . We need to get the values of  $Q$  and its tangential derivative at  $(x_{ij}^*, y_j)$ . We first reconstruct the interface in the local coordinates as  $\xi \approx C\eta^2 + D\eta^3$  with error  $O(\eta^4)$ . We refer the readers to section 11.1.5 in [43] on how to find  $C$  and  $D$ . We then approximate  $Q(\eta)$  as  $Q(\eta) = Q_k + \omega_1\eta + \omega_2\eta^2$  locally with error  $O(\eta^3)$  and  $Q'(\eta) = \omega_1 + 2\omega_2\eta$  with error  $O(\eta^2)$ . The coefficients  $\omega_1$  and  $\omega_2$  are determined from  $Q$  values at the two closest orthogonal projections.

**4.2.1. The finite difference scheme at a regular grid point.** At a regular grid point  $(x_i, y_j)$ , the finite difference scheme is the classic conservative one with the scaling

$$(4.12) \quad \frac{\beta_{i-1/2,j}U_{i-1,j} + \beta_{i+1/2,j}U_{i+1,j} + \beta_{i,j-1/2}U_{i,j-1} + \beta_{i,j+1/2}U_{i,j+1} - \bar{\beta}_{ij}U_{i,j}}{h^2\bar{\beta}_{ij}} = \frac{f_{ij}}{\bar{\beta}_{ij}},$$

where  $f_{ij} = f(x_i, y_j)$ ,  $\beta_{i-1/2,j} = \beta(x_i - h/2, y_j)$ , and so on, and

$$(4.13) \quad \bar{\beta}_{ij} = \beta_{i-1/2,j} + \beta_{i+1/2,j} + \beta_{i,j-1/2} + \beta_{i,j+1/2}.$$

**4.2.2. The finite difference scheme at an irregular grid point.** We assume that we know the jump conditions  $[u] = w$  and  $[u_n] = q$ , not the original flux jump condition  $[\beta u_n] = v$ . This makes it easier to derive accurate and stable finite difference schemes. At an irregular grid point, we discretize the rewritten equation (4.1) using a dimension by dimension approach, and an upwinding discretization for the first order derivative terms.

Let  $(x_i, y_j)$  be an irregular grid point. If the interface does not cut through the interval  $(x_{i-1}, x_{i+1})$  along the line  $y = y_j$ , that is,  $(x_i, y_j)$  is regular in the  $x$ -direction, then the finite difference approximation for  $(\beta u_x)_x$  before the scaling is

$$(4.14) \quad (\beta u_x)_x \approx \frac{\beta_{i-1/2,j}U_{i-1,j} + \beta_{i+1/2,j}U_{i+1,j} - (\beta_{i-1/2,j} + \beta_{i+1/2,j})U_{i,j}}{h^2}.$$

The final finite difference equation will be scaled similarly to those at regular grid points.

Now assume the interface cuts the grid line  $y(x) = y_j$  in the interval  $(x_{i-1}, x_{i+1})$ , say at  $(x_{ij}^*, y_j)$ , with  $x_{ij}^* = x_i + \alpha_{ij}^x h$ ,  $0 \leq |\alpha_{ij}^x| < 1$ . Without loss of generality, we assume that  $(x_i, y_j) \in \Omega^-$ . We discretize the reformulated equation (4.1), that is,

$$(4.15) \quad u_{xx}^- + u_{yy}^- + \frac{\beta_x^- u_x^-}{\beta^-} + \frac{\beta_y^- u_y^-}{\beta^-} = \frac{f^-}{\beta^-},$$

where  $f^-$ ,  $\beta^-$ , ... are the limiting values at  $(x_{ij}^*, y_j)$  from the  $\Omega^-$  side. We use an upwinding scheme for the first order term  $\beta_x^- u_x^- / \beta^-$ , that is,

$$(4.16) \quad \frac{\beta_x^- u_x^-}{\beta^-} \approx \begin{cases} \frac{\beta_x^-}{\beta^-} \left( \frac{U_{i,j} - U_{i-1,j}}{h} + \frac{\tilde{C}_{ij}^x}{h} \right) & \text{if } \frac{\beta_x^-}{\beta^-} \leq 0, \\ \frac{\beta_x^-}{\beta^-} \left( \frac{U_{i+1,j} - U_{i,j}}{h} + \frac{\tilde{C}_{ij}^x}{h} \right) & \text{otherwise,} \end{cases}$$

where, for example,  $\tilde{C}_{ij}^x = 0$  if  $(x_{i-1}, y_j) \in \Omega^-$ . Otherwise we have

$$(4.17) \quad \tilde{C}_{ij}^x = - \left( [u] + [u_x] (1 - |\alpha_{ij}^x|) h \right), \quad \text{where} \quad \alpha_{ij}^x = \frac{x_{ij}^* - x_i}{h};$$

see Lemma 10.6 in [43] for the formulas of the correction, where the jumps again are defined at  $(x_{ij}^*, y_j)$ . Similarly, for the second order term  $u_{xx}$ , the finite difference approximation for  $u_{xx}$  can be written as

$$(4.18) \quad u_{xx}^-(x_i, y_j) \approx \frac{U_{i-1,j} - 2U_{i,j} + U_{i+1,j} - C_{ij}^x}{h^2},$$

where the correction term  $C_{ij}^x$  is

$$(4.19) \quad C_{ij}^x = [u] + [u_x] (1 - |\alpha_{ij}^x|) h + [u_{xx}] \frac{(1 - |\alpha_{ij}^x|)^2 h^2}{2}.$$

**4.2.3. Approximating  $[u_{xx}]$  and  $[u_{yy}]$ .** Given  $[u] = w$  and  $[u_n] = q$  along the interface, from (4.7) and (4.6) we have

$$\begin{aligned} [u_x] &= \cos \theta [u_\xi] - \sin \theta [u_\eta] = q \cos \theta - w' \sin \theta, \\ [u_y] &= \sin \theta [u_\xi] + \cos \theta [u_\eta] = q \sin \theta + w' \cos \theta, \\ [u_{xx}] &= \cos^2 \theta [u_{\xi\xi}] - 2 \sin \theta \cos \theta [u_{\xi\eta}] + \sin^2 \theta [u_{\eta\eta}] \\ &= -2 \sin \theta \cos \theta (w' \chi'' + q') + \sin^2 \theta (-q \chi'' + w'') \\ &\quad + \cos^2 \theta \left\{ q \left( \chi'' - \frac{\beta_\xi^+}{\beta^+} \right) - w'' - \frac{\beta_\eta^+}{\beta^+} w' + \left[ \frac{f}{\beta} \right] \right. \\ &\quad \left. - \left[ \frac{\beta_\xi}{\beta} \right] (\cos \theta u_x^- + \sin \theta u_y^-) - \left[ \frac{\beta_\eta}{\beta} \right] (-\sin \theta u_x^- + \cos \theta u_y^-) \right\}, \\ [u_{yy}] &= \sin^2 \theta [u_{\xi\xi}] + 2 \sin \theta \cos \theta [u_{\xi\eta}] + \cos^2 \theta [u_{\eta\eta}] \\ &= 2 \sin \theta \cos \theta (w' \chi'' + q') + \cos^2 \theta (-q \chi'' + w'') \\ &\quad + \sin^2 \theta \left\{ q \left( \chi'' - \frac{\beta_\xi^+}{\beta^+} \right) - w'' - \frac{\beta_\eta^+}{\beta^+} w' + \left[ \frac{f}{\beta} \right] \right. \\ &\quad \left. - \left[ \frac{\beta_\xi}{\beta} \right] (\cos \theta u_x^- + \sin \theta u_y^-) - \left[ \frac{\beta_\eta}{\beta} \right] (-\sin \theta u_x^- + \cos \theta u_y^-) \right\}, \end{aligned}$$

where  $w'$  and  $q'$  are the first order derivatives and  $w''$  is the second order derivative along the interface, respectively. In the derivation above, we have used formulas

$$(4.20) \quad u_\xi = u_x \cos \theta + u_y \sin \theta, \quad u_y = -u_x \sin \theta + u_y \cos \theta.$$

Most of the terms in  $[u_{xx}]$  and  $[u_{yy}]$  are computable except terms of  $u^-$ ,  $u_x^-$ , and  $u_y^-$ . Note that these functions are defined on the interface. Using Taylor expansion, we have  $u^-(X, Y) = u^-(x_i, y_j) + O(h)$ ,  $u_x^-(X, Y) = u_x^-(x_i, y_j) + O(h)$ , and  $u_y^-(X, Y) = u_y^-(x_i, y_j) + O(h)$ . We simply replace  $u^-$  with  $U_{ij}$  and treat  $u_x^-$  and  $u_y^-$  using the upwinding scheme to increase the diagonal dominance of the resulting linear system

of finite difference equations. For example, for the terms containing  $u_x^-$  in  $[u_{xx}]$  we use

$$\left( \left[ \frac{\beta_\eta}{\beta} \right] \sin \theta - \left[ \frac{\beta_\xi}{\beta} \right] \cos \theta \right) \cos^2 \theta u_x^- = \begin{cases} A_{tmp} \left( \frac{U_{i+1,j} - U_{i,j}}{h} + \frac{\tilde{C}_{ij}^x}{h} \right) & \text{if } A_{tmp} \geq 0, \\ A_{tmp} \left( \frac{U_{i,j} - U_{i-1,j}}{h} + \frac{\tilde{C}_{ij}^x}{h} \right) & \text{otherwise,} \end{cases}$$

$$\text{where } A_{tmp} = \left( \left[ \frac{\beta_\eta}{\beta} \right] \sin \theta - \left[ \frac{\beta_\xi}{\beta} \right] \cos \theta \right) \cos^2 \theta,$$

and once again, for example,  $\tilde{C}_{ij}^x = 0$  if  $(x_{i-1}, y_j) \in \Omega^-$ . Otherwise,

$$(4.21) \quad \tilde{C}_{ij}^x = - \left( [u] + [u_x] (1 - |\alpha_{ij}^x|) h \right).$$

The linear system of finite difference equations can be written as

$$(4.22) \quad A_h \mathbf{U} + B \mathbf{Q} = \mathbf{F}_1,$$

where  $\mathbf{U}$  is the vector formed by the finite difference approximation  $\{U_{ij}\}$  to the solution  $\{u(x_i, y_j)\}$ ,  $\mathbf{Q}$  is the vector formed by the discrete augmented variable  $\{Q_k\}$  to the augmented variable  $\{[\frac{\partial u}{\partial n}(X_k, Y_k)]\}$ ,  $\mathbf{F}_1$  is the modified right-hand side, and  $B$  is a sparse matrix corresponding to the correction terms for the  $[u_n]$  term.

*Remark 4.2.*

- The finite difference stencil is still standard five-point centered. This is different from the maximum principal preserving scheme [42] in which the finite difference stencil is nine-point.
- $A_h$  is an M-matrix and irreducible, and thus it is invertible. No optimization is needed compared to that in [42] because we assume that  $[u_n]$  is given instead of  $[\beta u_n]$ , which makes it easier to discretize the interface problem. The trade-off is that we also need to solve the augmented variable.

**4.3. Discretizing the flux jump condition.** At every approximate orthogonal projection of all irregular grid points on the interface, we use the same least squares interpolation described in section 4 in [39] to interpolate the flux jump condition  $[\beta u_n] = v$ .

At one orthogonal projection  $\mathbf{X}_k = (X_k, Y_k)$  corresponding to an irregular grid point  $(x_i, y_j)$ , the second order accurate least squares interpolation scheme approximating  $[\beta u_n] = v$  can be written as

$$(4.23) \quad \sum_{|\mathbf{x}_{ij} - \mathbf{X}_k| \leq \delta_h} \gamma_{ij} U_{ij} + L_k(\beta(\mathbf{x}), \mathbf{W}, \mathbf{Q}, \mathbf{V}) = 0,$$

where  $\delta_h$  is a parameter of  $2h \sim 3h$ ,  $L_k$  stands for a linear relation of its arguments  $w(\mathbf{X})$ ,  $q(\mathbf{X})$ , and  $v(\mathbf{X})$  in discrete form. The consistency condition requires that

$$(4.24) \quad \sum_{|\mathbf{x}_{ij} - \mathbf{X}_k| \leq \delta_h} \gamma_{ij} = 0.$$

Note that the interpolation coefficients should depend on the index  $k$  as well; we omit them for simplicity of notation.

In the matrix-vector form, the interpolation at all projections of irregular grid points from one particular side can be written as

$$(4.25) \quad S\mathbf{U} + G\mathbf{Q} = \mathbf{F}_2$$

for some sparse matrices  $S$  and  $G$ . If we put (4.22) and (4.25) together, we get

$$(4.26) \quad \begin{bmatrix} A_h & B \\ S & G \end{bmatrix} \begin{bmatrix} \mathbf{U} \\ \mathbf{Q} \end{bmatrix} = \begin{bmatrix} \mathbf{F}_1 \\ \mathbf{F}_2 \end{bmatrix}.$$

Eliminating  $U$  in (4.26) gives the Schur complement equation for  $\mathbf{Q}$ ,

$$(4.27) \quad (G - SA_h^{-1}B)\mathbf{Q} = \mathbf{F}_2 - SA_h^{-1}\mathbf{F}_1 \quad \text{or} \quad A_h^{schur}\mathbf{Q} = \mathbf{F}^{schur}.$$

We use the GMRES iterative method to solve the Schur complement system and do not explicitly form the matrices  $A_h$ ,  $B$ ,  $S$ ,  $G$ , and  $A_h^{schur}$ . The matrix and vector multiplication  $A_h^{schur}\mathbf{Q}$  needed for the GMRES iteration involves two consecutive steps: the first step is to solve the interface problem (4.22) given  $\mathbf{Q}$ , and the second step is to find the residual of the flux jump condition, that is,  $R(\mathbf{Q}) = [\beta(\mathbf{X})\mathbf{U}_n(\mathbf{Q})] - \mathbf{V}$ . We refer the reader to section 5.1 in [39] for details.

**4.4. Computing the gradient on the interface.** At one orthogonal projection  $\mathbf{X}_k$  corresponding to an irregular grid point  $(x_i, y_j)$ , we use a similar (two-sided SVD) interpolation to approximate the normal derivative at  $\mathbf{X}_k$  from the  $\Omega^-$  side,

$$(4.28) \quad u_n^-(\mathbf{X}_k) = \sum_{|\mathbf{x}_{ij} - \mathbf{X}_k| \leq \delta_h} \widetilde{\gamma}_{ij} U_{ij} + \widetilde{L}_k(\beta(\mathbf{x}), \mathbf{W}, \mathbf{Q}, \mathbf{V}),$$

to get one of  $u_n^-(\mathbf{X}_k)$  or  $u_n^+(\mathbf{X}_k)$ , and then we use  $q(\mathbf{X}_k)$  to get the other, say  $u_n^+(\mathbf{X}_k) = q(\mathbf{X}_k) + u_n^-(\mathbf{X}_k)$ . The linear system of equations has the same coefficient matrix as that in (4.23) for  $\gamma_{ij}$ 's, so there is almost no additional cost. The term  $\widetilde{L}_k(\beta(\mathbf{x}), \mathbf{W}, \mathbf{Q}, \mathbf{V})$  is again a correction term due to the jumps in the involved quantities.

If needed, at a grid point the partial derivatives  $u_x$  and  $u_y$  can be calculated using the standard three-point central finite difference formula with (at an irregular grid point) or without (at a regular grid point) a correction term. Beale and Layton [8] showed that the computed derivatives using the IIM are second order accurate in the  $L^\infty$  norm at all grid points.

**4.5. A new preconditioning strategy.** The number of GMRES iterations grows linearly with the mesh size  $N$  if there is no preconditioning technique employed. The preconditioning technique proposed in [39] works well for a piecewise constant coefficient but not for a variable coefficient. The idea of a new preconditioning technique is more like a diagonal preconditioning technique for the Schur complement. At an orthogonal projection  $\mathbf{X}_k = (X_k, Y_k)$  where the augmented variable is defined, we use the rescaled residual of the flux jump condition

$$(4.29) \quad R^{rescaled}(\mathbf{X}_k) = \frac{\beta^+(\mathbf{X}_k)U_n^+(\mathbf{X}_k) - \beta^-(\mathbf{X}_k)U_n^-(\mathbf{X}_k) - v(\mathbf{X}_k)}{\bar{\beta}(\mathbf{X}_k)},$$

where  $\bar{\beta}(\mathbf{X}_k) = (\beta^-(\mathbf{X}_k) + \beta^+(\mathbf{X}_k))/2$ , to discretize the flux jump condition.



**5. Convergence proof for the 2D problems.** In this section, we provide a convergence proof for 2D problems. For simplicity, we assume that a Dirichlet boundary condition is prescribed along the boundary  $\partial\Omega$ . We use  $\mathbf{U}$  and  $\mathbf{u}$  to represent the vectors of approximate and exact solutions at grid points;  $\mathbf{T}^u$  and  $\mathbf{E}^u = \mathbf{U} - \mathbf{u}$  are the vectors of the local truncation errors and the global error. We have  $\mathbf{E}^u|_{\partial\Omega_h} = \mathbf{0}$  for the values at grid points on the boundary. Similarly, we define  $\mathbf{T}^q$  and  $\mathbf{E}^q = \mathbf{Q} - \mathbf{q}$  as the vectors of the local truncation error and the global error for the augmented variable. According to the definition, we have

$$(5.1) \quad A_h \mathbf{U} + B\mathbf{Q} = \mathbf{F}_1, \quad A_h \mathbf{E}^u + B\mathbf{E}^q = \mathbf{T}^u,$$

$$(5.2) \quad S\mathbf{U} + G\mathbf{Q} = \mathbf{F}_2, \quad S\mathbf{E}^u + G\mathbf{E}^q = \mathbf{T}^q,$$

where the local truncation error vector  $\mathbf{T}^u$  is defined as  $\mathbf{T}^u = \mathbf{F}_1 - A_h \mathbf{u} - B\mathbf{q}$  and so on.

**LEMMA 5.1.** *Assume that  $u(\mathbf{x})$  is in piecewise  $C^4(\Omega \setminus \Gamma)$  excluding the interface  $\Gamma$ . If the augmented variable is a second order approximation to  $[\frac{\partial u}{\partial n}(\mathbf{X})]$ , that is,  $\|\mathbf{E}^q\|_\infty \leq Ch^2$ , then the computed solution of the finite difference equations (4.22) is also second order accurate, that is,  $\|\mathbf{E}\|_\infty \leq Ch^2$ .*

*Proof.* From the construction of the numerical scheme we know that a component of  $B\mathbf{E}^q$  is zero at a regular grid point  $\mathbf{x}_{ij}$  and bounded by  $Ch$  at an irregular grid point  $\mathbf{x}_{ij}$ , since  $\|\mathbf{E}^q\|_\infty \leq Ch^2$  as one of the conditions in the theorem. Note that  $A_h$  is an M-matrix and  $A_h \mathbf{E}^u = -B\mathbf{E}^q + \mathbf{T}^u$  in which  $\mathbf{T}^u$  is bounded by  $Ch^2$  at regular grid points and  $Ch$  at irregular grid points. From Theorem 3.3 in [43] or the convergence analysis of IIM in [8], we conclude that the global error is bounded by  $Ch^2$ . Also from [57, 58], the partial derivatives using the IIM are also second order accurate.  $\square$

The next part is to show that the computed augmented variable is also second order accurate by a factor of  $\log h$ . In this case, we first assume that the coefficient is piecewise constant so that we can apply some theoretical results from [41].

**THEOREM 5.2.** *Assume that  $u(\mathbf{x})$  is in piecewise  $C^4(\Omega \setminus \Gamma)$ , excluding the interface  $\Gamma$ , and that the coefficient  $\beta(\mathbf{x})$  is a piecewise constant  $\beta^-$  and  $\beta^+$ ; then the computed augmented variable is second order accurate by the fact of  $|\log h|$ , that is,  $\|\mathbf{E}^q\|_\infty \leq Ch^2 |\log h|$ .*

*Proof.* From (5.1)–(5.2), we have

$$(5.3) \quad (G - SA_h^{-1}B) \mathbf{E}^q = -\mathbf{T}^q + SA_h^{-1}\mathbf{T}^u.$$

Note that solvability of the above linear system is shown in [39]. We first prove that the right-hand side above is bounded by  $Ch^2$ . Since the interpolation for the flux jump condition is second order, we have  $\|\mathbf{T}^q\|_\infty \leq Ch^2$ . For the second term, from the interpolation scheme in (4.23), we consider one component and carry out the

derivation

$$\begin{aligned}
 (SA_h^{-1}\mathbf{T}^u)_k &= \sum_{|\mathbf{x}_{ij}-\mathbf{X}_k|\leq\delta_h} \gamma_{ij} (A_h^{-1}\mathbf{T}^u)_{ij} \\
 &= \sum_{|\mathbf{x}_{ij}-\mathbf{X}_k|\leq\delta_h} \gamma_{i,j} \sum_{l,r} G^h(\mathbf{x}_{lr}, \mathbf{x}_{ij}) h^2 \tau_{lr} \\
 &= \sum_{l,r} h^2 \tau_{lr} \left( \sum_{|\mathbf{x}_{ij}-\mathbf{X}_k|\leq\delta_h} \gamma_{i,j} G^h(\mathbf{x}_{lr}, \mathbf{x}_{ij}) \right),
 \end{aligned}
 \tag{5.4}$$

where  $G^h(\mathbf{x}_{lr}, \mathbf{x}_{ij})$  is the discrete Green function defined as

$$\mathbf{G}^h(\mathbf{x}_{ij}, \mathbf{x}_{lm}) = \left( A_h^{-1} \mathbf{e}_{lm} \frac{1}{h^2} \right)_{ij}, \quad \mathbf{G}^h(\partial\Omega_h, \mathbf{x}_{lm}) = 0,
 \tag{5.5}$$

where  $\mathbf{e}_{lm}$  is the unit grid function whose values are zero at all grid points except at  $\mathbf{x}_{lm} = (x_l, y_m)$  where its component is  $e_{lm} = 1$ ; see, for example, [21]. Note that in the neighborhood of  $|\mathbf{x}_{ij} - \mathbf{X}_k| \leq \delta_h$ , the points involved in the interpolation are close to  $\mathbf{X}_k$ ; we can continue to derive

$$\begin{aligned}
 (SA_h^{-1}\mathbf{T}^u)_k &= \sum_{l,r} h^2 \tau_{lr} \left( \sum_{|\mathbf{x}_{ij}-\mathbf{X}_k|\leq\delta_h} \gamma_{i,j} \left( G_I^h(\mathbf{x}_{lr}, \mathbf{X}_k) + h \frac{G^h(\mathbf{x}_{lr}, \mathbf{x}_{ij}) - G_I^h(\mathbf{x}_{lr}, \mathbf{X}_k)}{h} \right) \right) \\
 &= \sum_{l,r} h^2 \tau_{lr} \left( \sum_{|\mathbf{x}_{ij}-\mathbf{X}_k|\leq\delta_h} \gamma_{i,j} G_I^h(\mathbf{x}_{lr}, \mathbf{X}_k) \right) \\
 &\quad + \sum_{l,r} h^3 \tau_{lr} \left( \sum_{|\mathbf{x}_{ij}-\mathbf{X}_k|\leq\delta_h} \gamma_{i,j} \left( \frac{\partial G_I^h(\mathbf{x}_{lr}, \mathbf{X}_k)}{\partial \mathbf{x}} \right) + O(h) \right) \\
 &= \sum_{l,r} h^3 \tau_{lr} \left( \sum_{|\mathbf{x}_{ij}-\mathbf{X}_k|\leq\delta_h} \gamma_{i,j} \left( \frac{\partial G_I^h(\mathbf{x}_{lr}, \mathbf{X}_k)}{\partial \mathbf{x}} \right) + O(h) \right).
 \end{aligned}$$

The first term in the first line of this equation is zero due to the consistency of the interpolation scheme for the flux jump condition. We have  $|\tau_{lr}| \leq Ch^2$  at regular grid points and  $|\tau_{lr}| \leq Ch$  at irregular grid points, and from the estimate of  $\frac{\partial G_I^h}{\partial \mathbf{x}}$  in (3.16)

in [41] we further derive

$$\begin{aligned}
|(SA_h^{-1}\mathbf{T}^u)_k| &\leq \sum_{l,r} h^3 |\tau_{lr}| \left( \sum_{|\mathbf{x}_{ij}-\mathbf{X}_k|\leq\delta_h} |\gamma_{ij}| \left( \frac{C}{(\|\mathbf{x}_{lr}-\mathbf{X}_k\|_2+h)} \right) + O(h) \right) \\
&\leq \sum_{l,r,\Omega_h^{reg}} h^3 |\tau_{lr}| \left( \sum_{|\mathbf{x}_{ij}-\mathbf{X}_k|\leq\delta_h} |\gamma_{ij}| \left( \frac{C}{(\|\mathbf{x}_{lr}-\mathbf{X}_k\|_2+h)} \right) + O(h) \right) \\
&\quad + \sum_{l,r,\Omega_h^{irr}} h^3 |\tau_{lr}| \left( \sum_{|\mathbf{x}_{ij}-\mathbf{X}_k|\leq\delta_h} |\gamma_{ij}| \left( \frac{C}{(\|\mathbf{x}_{lr}-\mathbf{X}_k\|_2+h)} \right) + O(h) \right) \\
&\leq \sum_{l,r,\Omega_h^{reg}} h^4 \left( \sum_{|\mathbf{x}_{ij}-\mathbf{X}_k|\leq\delta_h} \left( \frac{C}{(\|\mathbf{x}_{lr}-\mathbf{X}_k\|_2+h)} \right) + O(h) \right) \\
&\quad + \sum_{l,r,\Omega_h^{irr}} h^3 \left( \sum_{|\mathbf{x}_{ij}-\mathbf{X}_k|\leq\delta_h} \left( \frac{C}{(\|\mathbf{x}_{lr}-\mathbf{X}_k\|_2+h)} \right) + O(h) \right) \\
&\leq h^2 \sum_{|\mathbf{x}_{ij}-\mathbf{X}_k|\leq\delta_h} \left( \sum_{l,r,\Omega_h^{reg}} \left( \frac{C}{(\|\mathbf{x}_{lr}-\mathbf{X}_k\|_2+h)} \right) h^2 + O(h^3) \right) \\
&\quad + h^2 \sum_{|\mathbf{x}_{ij}-\mathbf{X}_k|\leq\delta_h} \left( \sum_{l,r,\Omega_h^{irr}} \left( \frac{C}{(\|\mathbf{x}_{lr}-\mathbf{X}_k\|_2+h)} \right) h + O(h^3) \right) \\
&\leq Ch^2 |\log h| + Ch^2,
\end{aligned}$$

where  $\Omega_h^{irr}$  and  $\Omega_h^{reg}$  are the sets of all irregular and regular grid points, respectively. In the derivation above we have used the facts that  $|\gamma_{ij}| \sim 1/h$ ,  $|\tau_{lr}| \leq Ch^2$  at regular grid points and  $|\tau_{lr}| \leq Ch$  at irregular grid points, respectively. We have also used the estimate of the Riemann sum for the double integral  $\iint 1/(x^2+y^2+h) dx dy \leq C|\log h|$ . Note also that the total number of regular grid points is  $O(1/h^2)$ , while the total number of irregular grid points is  $O(1/h)$ . It has been shown that Schur complement matrix  $A_h^{schur}$  is nonsingular, and thus we have  $\|A_h^{schur}\mathbf{E}^q\|_\infty \leq Ch^2|\log h|$ .

We have shown that the right-hand side for the error of the augmented variable has the order of  $h^2 \log h$ . From section 6.1.2 in [43], we know that the left-hand side of (5.3) is

$$(5.6) \quad A_h^{schur}\mathbf{E}^q = \left[ \beta \frac{\partial \tilde{\mathbf{U}}}{\partial n}(\mathbf{E}^q) \right] - \left[ \beta \frac{\partial \tilde{\mathbf{U}}}{\partial n}(\mathbf{0}) \right],$$

where  $\tilde{\mathbf{U}}(\mathbf{E}^q)$  can be regarded as the solution of the numerical method applied to the problem

$$(5.7) \quad \nabla \cdot (\beta \nabla \tilde{u}) = \mathbf{T}_I^u(\mathbf{x}); \quad \tilde{u}|_{\partial\Omega} = 0,$$

$$(5.8) \quad [\tilde{u}]_\Gamma = 0, \quad \left[ \beta \frac{\partial \tilde{u}}{\partial n} \right]_\Gamma = \mathbf{T}_I^q(\mathbf{X}),$$

where  $\mathbf{T}_I^u(\mathbf{x}) \in C$  is an interpolation function of  $\mathbf{T}^u$  on the entire domain, while  $\mathbf{T}_I^q(\mathbf{X}) \in C$  is an interpolation function of  $\mathbf{T}^q$  along the interface. From the maximum

principle of elliptic PDEs, we know that  $|\tilde{u}| \leq Ch^2$  and  $|\frac{\partial \tilde{u}^\pm}{\partial n}| \leq Ch^2$ . Therefore the second term in (5.6) is bounded by  $Ch^2$ . Thus, we have

$$\begin{aligned} A_h^{schur} \mathbf{E}^q &= \left[ \beta \frac{\partial \tilde{\mathbf{U}}}{\partial n} (\mathbf{E}^q) \right] = \beta^+ \frac{\partial \tilde{\mathbf{U}}^+}{\partial n} (\mathbf{E}^q) - \beta^- \frac{\partial \tilde{\mathbf{U}}^-}{\partial n} (\mathbf{E}^q) + O(h^2) \\ &= \beta^+ \mathbf{E}^q - [\beta] \frac{\partial \tilde{\mathbf{U}}^-}{\partial n} (\mathbf{E}^q) + O(h^2). \end{aligned}$$

Since  $\beta$  is a piecewise constant that has been divided from both sides of the PDE (see (4.1)), from [8] we know that the solution and the derivative are both second order accurate when the IIM is applied, which implies that  $\|\frac{\partial \tilde{\mathbf{U}}^-}{\partial n} (\mathbf{E}^q)\|_\infty \leq Ch^2$ . We have already proved that  $\|A_h^{schur} \mathbf{E}^q\|_\infty \leq Ch^2$ ; this leads to  $\|\mathbf{E}^q\|_\infty \leq Ch^2$ .  $\square$

*Remark 5.3.* In the preconditioning strategy, we can write, for example, equation (6.24) in [43],

$$(5.9) \quad \frac{\partial \tilde{\mathbf{U}}^-}{\partial n} (\mathbf{E}^q) = \gamma \left[ \beta \frac{\partial \tilde{\mathbf{U}}^-}{\partial n} (\mathbf{E}^q) \right] + F_\Gamma + O(h^2),$$

where  $\gamma$  is a constant and  $F_\Gamma$  is a vector; then we have

$$\begin{aligned} A_h^{schur} \mathbf{Q} &= \left[ \beta \frac{\partial \mathbf{U}}{\partial n} (\mathbf{Q}) \right] - \left[ \beta \frac{\partial \mathbf{U}}{\partial n} (\mathbf{0}) \right] = \beta^+ \frac{\partial \mathbf{U}^+}{\partial n} (\mathbf{Q}) - \beta^- \frac{\partial \mathbf{U}^-}{\partial n} (\mathbf{Q}) - \left[ \beta \frac{\partial \mathbf{U}}{\partial n} (\mathbf{0}) \right] \\ &= (\beta^+ - \beta^- \gamma) \mathbf{Q} - \beta^- F_\Gamma - \left[ \beta \frac{\partial \mathbf{U}}{\partial n} (\mathbf{0}) \right] + O(h^2), \end{aligned}$$

which means that the Schur complement matrix is nearly a diagonal. This may explain why the number of the GMRES iterations is independent of the mesh size and the jump in  $\beta$ . For variable coefficient  $\beta(\mathbf{x})$ , with the new preconditioning strategy, we would have

$$A_h^{schur} \mathbf{Q} = D(\bar{\beta}(\mathbf{x})) \mathbf{Q} + \tilde{\mathbf{F}}_\Gamma + O(h^2),$$

where  $D(\bar{\beta}(\mathbf{x}))$  is a diagonal matrix whose entries are  $(\beta_k^+ - \beta_k^-)/\bar{\beta}_k$ ,  $\bar{\beta}_k = (\beta_k^+ + \beta_k^-)/2$ .

*Remark 5.4.* While the proof above is for a piecewise constant coefficient, the conclusion is also true—at least asymptotically in terms of  $h$ —for variable coefficient  $\beta(\mathbf{x}) \geq \beta_0 > 0$ —assuming that  $\beta(\mathbf{x}) \in C^\infty(\Omega^\pm)$ , since those terms involved are lower order terms of  $h$ . This is because the coefficient matrix  $A_h(\beta) = A_h(I + B_h)$  and  $\|B_h\| \rightarrow 0$  as  $h \rightarrow 0$ , where  $A_h$  is the discrete Laplacian. This is another advantage of using the reformulated PDE.

**6. Numerical examples.** We present a variety of numerical experiments to show the performance of the new augmented method for accurate solutions and its first order gradient at the interface. All the experiments are computed with double precision and are performed on a desktop computer with a Pentium Dual-Core CPU, 2.59 GHz, and 4GB memory. We also list the CPU time(s) in Tables 2–8. We present errors in  $L^\infty$  norms and estimate the convergence order using

$$r = \frac{1}{\log 2} \log \frac{\|\mathbf{E}_{2h}\|_\infty}{\|\mathbf{E}_h\|_\infty}.$$

The tolerance of the GMRES iteration is set to be  $10^{-6}$ , and the initial value is set to be  $\mathbf{0}$  in all computations. In Tables 2–8, “Iter” represents the number of GMRES iterations, “ $N_b$ ” the number of control points, “ $N$ ” the number of the grid lines in each direction of the rectangular domain, and “CPU(s)” the run time in seconds.

*Example 6.1.*

$$(6.1) \quad u(\mathbf{x}) = \begin{cases} \sin(x+y) & \text{in } \Omega^-, \\ \log(x^2 + y^2) & \text{in } \Omega^+, \end{cases} \quad \beta(\mathbf{x}) = \begin{cases} \sin(x+y) + 2 & \text{in } \Omega^-, \\ \cos(x+y) + 2 & \text{in } \Omega^+, \end{cases}$$

where the interface is the zero level set of  $\varphi(x, y) = \sqrt{x^2 + y^2} - 0.5$ , and  $\Omega = [-1, 1] \times [-1, 1]$ . The source term is  $f(\mathbf{x})$ , and the interface jump conditions  $[u]$  and  $[\beta u_n]$  are derived from the exact solution.

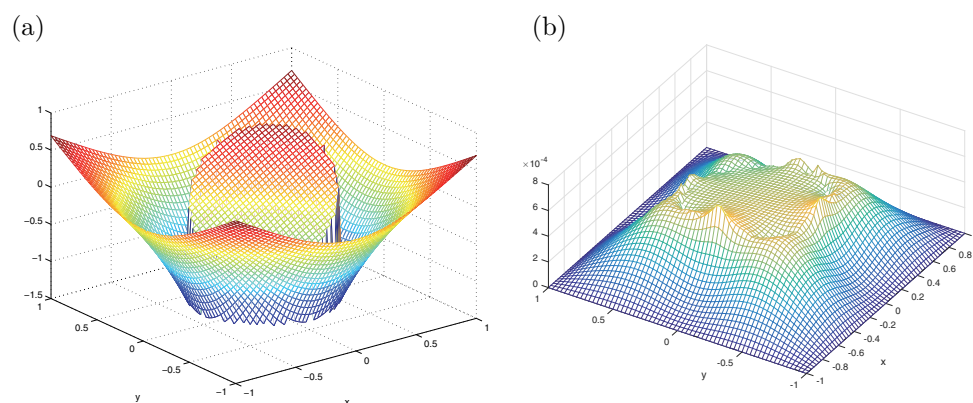


FIG. 3. (a) The solution plot of Example 6.1. (b) The error plot of the computed solution. The error seems to be piecewise smooth as well which is important for accurate gradient computation.

This is an almost arbitrary example with a genuine piecewise smooth nonlinear solution, and a variable coefficient with a variable discontinuity along the interface. We present a grid refinement analysis in Table 2. The second column is the maximum error of the solution, while the third column is the approximate convergence order. The fourth and sixth columns are the errors of the normal derivatives at the interface from the  $\Omega^-$  and  $\Omega^+$  sides, respectively. The fifth and seventh columns show the approximate convergence order of the computed normal derivative. The eighth column is the number of GMRES iterations, and the next-to-last column shows orthogonal projections of irregular grid points from the  $\Omega^+$  side. The last column is the total CPU time in seconds. We can observe from Table 2 that the new augmented IIM is second order accurate in both the solution globally and the gradient at the interface from each side. The total CPU time also shows that the method is very fast with the optimal computational complexity ( $O(N^2) \log(N^2)$ ). We also observe that the number of GMRES iterations is a constant independent of the mesh size. In Figure 3, we show one mesh plot of the computed solution (left), and the error (right).

Now we use the same solution and interface but with a large jump in the coefficient along the interface:

$$(6.2) \quad \beta(\mathbf{x}) = \begin{cases} 10e^{10x} & \text{in } \Omega^-, \\ \sin(x+y) + 2 & \text{in } \Omega^+. \end{cases}$$

TABLE 2

A grid refinement analysis for Example 6.1 with a modest variable jump in the coefficient.

$N$	$E(u)$	$r$	$E(u_n^-)$	$r$	$E(u_n^+)$	$r$	Iter	$N_b$	CPU(s)
32	$3.1245 \times 10^{-3}$		$1.5905 \times 10^{-2}$		$2.1712 \times 10^{-2}$		4	48	0.01
64	$7.0327 \times 10^{-4}$	2.15	$4.4752 \times 10^{-3}$	1.82	$5.5256 \times 10^{-3}$	1.97	4	92	0.03
128	$1.1565 \times 10^{-4}$	2.60	$1.1182 \times 10^{-3}$	2.00	$1.3993 \times 10^{-3}$	1.98	4	184	0.11
256	$2.7720 \times 10^{-5}$	2.06	$2.9096 \times 10^{-4}$	1.94	$3.7998 \times 10^{-4}$	1.88	4	364	0.46
512	$6.2087 \times 10^{-6}$	2.15	$7.3489 \times 10^{-5}$	1.98	$9.8004 \times 10^{-5}$	1.95	4	728	2.45

The jump ratio varies from 1 : 10 to 1.45 : 1482 along the interface, a quite dramatic change. The results are shown in Table 3. We observe that the errors are larger than those in Table 2. This is due to the variations of the coefficient. Since the rescaled PDE has the form  $\Delta u + \frac{1}{\beta} \nabla \beta(x) \cdot \nabla u + \dots$ , we would expect the error term to contain  $\frac{\beta_x}{\beta} u_x$  and  $\frac{\beta_y}{\beta} u_y$  that are  $O(1)$  for Table 2 and  $O(10^2)$  for Table 3 due to the term  $10e^{10x}$ . This is the reason for the difference in the errors. Nevertheless, all the nice features are the same as those in the previous example.

TABLE 3

A grid refinement analysis for Example 6.1 with a large variation in the jump ratio of the coefficient.

$N$	$E(u)$	$r$	$E(u_n^-)$	$r$	$E(u_n^+)$	$r$	Iter	$N_b$	CPU(s)
32	$6.0115 \times 10^{-1}$		3.9014		1.7570		11	48	0.02
64	$1.4706 \times 10^{-1}$	2.03	$8.6974 \times 10^{-1}$	2.16	$4.2479 \times 10^{-1}$	2.04	10	92	0.07
128	$4.3411 \times 10^{-2}$	1.76	$2.5265 \times 10^{-1}$	1.78	$1.2537 \times 10^{-1}$	1.76	10	184	0.27
256	$1.1266 \times 10^{-2}$	1.94	$6.5293 \times 10^{-2}$	1.95	$3.2493 \times 10^{-2}$	1.94	10	364	1.24
512	$2.9178 \times 10^{-3}$	1.94	$1.6916 \times 10^{-2}$	1.94	$8.4205 \times 10^{-3}$	1.94	10	728	7.85

**An example with more general jump conditions.** There are some applications in which we may have more general jump conditions. Here we consider an example with a more general jump condition,  $c(\mathbf{X})u_n^+ - d(\mathbf{X})u_n^- = v(\mathbf{X})$  with  $c(\mathbf{X}) = x^2 + 1$ ,  $d(\mathbf{X}) = y^2 + 1$ . Our method still can work with the modified augmented equation (4.25) (now it is  $c(\mathbf{X})u_n^+ - d(\mathbf{X})u_n^- = v(\mathbf{X})$ ) and different preconditioning techniques. The convergence analysis may no longer apply directly. In Table 4, we list the grid refinement analysis which has the same predicted convergence and efficiency.

TABLE 4

A grid refinement analysis with a different jump condition  $c(\mathbf{X})u_n^+ - d(\mathbf{X})u_n^- = v(\mathbf{X})$ .

$N$	$E(u)$	$r$	$E(u_n^-)$	$r$	$E(u_n^+)$	$r$	Iter	$N_b$	CPU(s)
32	$1.0220 \times 10^{-2}$		$2.4784 \times 10^{-2}$		$2.5529 \times 10^{-2}$		4	48	0.047
64	$2.9257 \times 10^{-3}$	1.80	$6.5909 \times 10^{-3}$	1.91	$6.2884 \times 10^{-3}$	2.02	4	92	0.172
128	$7.9724 \times 10^{-4}$	1.87	$1.7941 \times 10^{-3}$	1.87	$1.5052 \times 10^{-3}$	2.06	4	184	0.578
256	$2.0781 \times 10^{-4}$	1.93	$4.6908 \times 10^{-4}$	1.93	$3.7353 \times 10^{-4}$	2.01	4	364	2.531
512	$5.3324 \times 10^{-5}$	1.96	$1.2033 \times 10^{-4}$	1.96	$9.5584 \times 10^{-5}$	1.96	4	728	10.141
1024	$1.3253 \times 10^{-5}$	2.00	$3.7729 \times 10^{-5}$	1.67	$3.0206 \times 10^{-5}$	1.66	4	1452	44.281

*Example 6.2. A general interface example with a piecewise constant coefficient.* This example is from [39]. The interface is the zero level set function

$$(6.3) \quad \varphi(\mathbf{x}) = r - (0.5 + 0.2 \sin(5\theta)),$$

and the true solution is

$$(6.4) \quad u(\mathbf{x}) = \begin{cases} \frac{r^2}{\beta^-}, & \mathbf{x} \in \Omega^-, \\ \frac{r^4 + C_0 \log(2r)}{\beta^+}, & \mathbf{x} \in \Omega^+. \end{cases}$$

The interface is both convex and concave and has relatively large curvature at some places; see Figure 1. We repeat this example with the new preconditioning technique with  $\beta^+ = 1000$  and  $\beta^- = 1$  on the domain  $\Omega = [-1, 1] \times [-1, 1]$ . The results are shown in Table 5 and are almost the same as those of the original fast IIM in [39]. Once again we observe that both the solution and the gradient are second order accurate, and the number of GMRES iterations is independent of the mesh size. For this example, the interface has large curvature at some places. We need a reasonable fine mesh to resolve the interface.

In Figure 4(a), we plot the computed solution of Example 6.2.

TABLE 5

A grid refinement analysis for Example 6.2 with a piecewise constant coefficient  $\beta^+ = 1000$  and  $\beta^- = 1$  and a complicated interface.

$N$	$E(u)$	$r$	$E(u_n^-)$	$r$	$E(u_n^+)$	$r$	Iter	$N_b$	CPU(s)
32	$1.2880 \times 10^{-1}$		3.0969		$3.0971 \times 10^{-3}$		14	78	0.04
64	$1.9431 \times 10^{-1}$	-0.59	4.0397	-0.38	$4.0396 \times 10^{-3}$	-0.38	14	154	0.13
128	$1.8734 \times 10^{-2}$	3.37	$4.9723 \times 10^{-1}$	3.02	$4.9765 \times 10^{-4}$	3.02	11	308	0.28
256	$2.3009 \times 10^{-3}$	3.02	$1.2096 \times 10^{-1}$	2.03	$1.2352 \times 10^{-4}$	2.01	10	612	0.99
512	$3.6351 \times 10^{-4}$	2.66	$2.2790 \times 10^{-2}$	2.40	$2.4786 \times 10^{-5}$	2.31	9	1226	21.50

**6.1. An example for more general self-adjoint elliptic interface problems.** With some modifications, the method developed in this paper has been generalized to more general interface problems

$$(6.5) \quad \nabla \cdot (\beta(\mathbf{x}) \nabla u(\mathbf{x})) - \sigma(\mathbf{x})u(\mathbf{x}) = f(\mathbf{x}).$$

The regularity requirement for the existence of the solution includes additional conditions  $\sigma(\mathbf{x}) \in C(\Omega^\pm)$  and  $\sigma(\mathbf{x}) \geq 0$ . While we still get second order accuracy both in the solution and the gradient, the coefficient matrix from the modified algorithm may no longer be an M-matrix. Nevertheless, the number of affected entries is  $O(1)$  compared with total  $O(1/h^2)$  when  $\sigma(\mathbf{x}) = 0$ , that is,  $A_h^{\sigma \neq 0} = A_h^{\sigma=0}(I + B_h)$  with  $\|B_h\| \leq Ch^2$ . Thus, we have asymptotically the same order of convergence as that in the case  $\sigma = 0$ .

*Example 6.3. A general example with  $\sigma(\mathbf{x}) \neq 0$ .* We present a more general example with a nonzero  $\sigma(\mathbf{x})$  term with different interfaces, an ellipse, and a five-star shaped curve. The true solution and coefficient are

$$(6.6) \quad u(\mathbf{x}) = \begin{cases} -x^3 + 2y^3 & \text{in } \Omega^-, \\ \sin(x+y) & \text{in } \Omega^+, \end{cases} \quad \beta(\mathbf{x}) = \begin{cases} 1 + e^{x+2y} & \text{in } \Omega^-, \\ \sin(2x-y) + 3 & \text{in } \Omega^+, \end{cases}$$

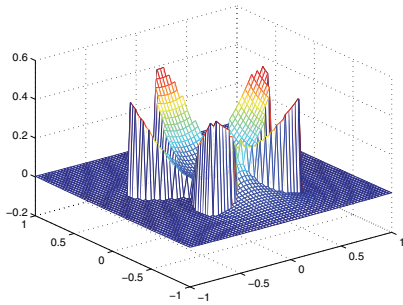
$$(6.7) \quad \sigma(\mathbf{x}) = \begin{cases} \cos(xy) + 2 & \text{in } \Omega^-, \\ x^2 + y^2 + 1 & \text{in } \Omega^+, \end{cases}$$

TABLE 6

A grid refinement analysis for Example 6.3 for a general elliptic interface problem with the interface  $(x/0.6)^2 + (y/0.4)^2 = 1$ .

$N$	$E(u)$	$r$	$E(u_n^-)$	$r$	$E(u_n^+)$	$r$	Iter	$N_b$	CPU(s)
32	$8.4180 \times 10^{-3}$		$9.0987 \times 10^{-2}$		$8.0826 \times 10^{-2}$		4	48	0.10
64	$9.0036 \times 10^{-4}$	3.22	$2.3473 \times 10^{-2}$	1.95	$1.9611 \times 10^{-2}$	2.04	4	96	0.20
128	$1.5842 \times 10^{-4}$	2.50	$4.1771 \times 10^{-3}$	2.49	$3.6921 \times 10^{-3}$	2.40	4	188	1.60
256	$3.7209 \times 10^{-5}$	2.09	$1.0639 \times 10^{-3}$	1.97	$9.4238 \times 10^{-4}$	1.97	4	372	3.02
512	$9.3380 \times 10^{-6}$	1.99	$3.2952 \times 10^{-4}$	1.69	$2.4187 \times 10^{-4}$	1.96	4	740	15.02

(a)



(b)

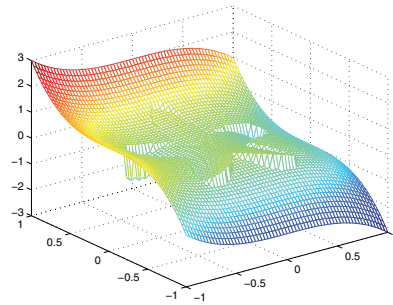


FIG. 4. (a) The computed solution plot of Example 6.2. (b) The solution plot of Example 6.3.

where again  $\Omega = [-1, 1] \times [-1, 1]$ . This is a very general example for a self-adjoint elliptic interface problem with nonlinear solution. We test our method for two different interfaces.

In Figure 4(b), we plot the computed solution of Example 6.3.

In Table 6, we show a grid refinement analysis for an elliptic interface  $\varphi(x, y) = (x/0.6)^2 + (y/0.4)^2 - 1$ . We observe once again second order convergence for the global solution and the gradient at the interface.

In Table 7, we show a grid refinement analysis for a skinny ellipse  $\varphi(x, y) = x^2 + (y/0.25)^2 - 1$  in the domain  $[-1.5, 1.5] \times [-1.5, 1.5]$ . Once we have the mesh fine enough to resolve the interface (here  $N \geq 64$ ), we observe once again second order convergence for the global solution and the gradient at the interface, although the largest error often appears near the tips of the longer axis of the ellipse.

TABLE 7

A grid refinement analysis for Example 6.3 for a general elliptic interface problem with the interface  $x^2 + (y/0.25)^2 = 1$ .

$N$	$E(u)$	$r$	$E(u_n^-)$	$r$	$E(u_n^+)$	$r$	Iter	$N_b$	CPU(s)
32	$8.2459 \times 10^{-2}$		1.3352		1.2700		5	44	0.078
64	$4.7769 \times 10^{-2}$	0.78	$8.9448 \times 10^{-1}$	0.57	$6.7590 \times 10^{-1}$	0.90	5	88	0.156
128	$6.5830 \times 10^{-3}$	2.85	$1.6557 \times 10^{-1}$	2.43	$1.5748 \times 10^{-1}$	2.10	5	176	1.250
256	$9.2772 \times 10^{-4}$	2.82	$7.1232 \times 10^{-2}$	1.21	$4.7413 \times 10^{-2}$	1.73	5	352	2.250
512	$1.7125 \times 10^{-4}$	2.43	$1.4364 \times 10^{-2}$	2.31	$1.1780 \times 10^{-2}$	2.00	5	704	19.703
1024	$4.5859 \times 10^{-5}$	1.90	$3.3351 \times 10^{-3}$	2.10	$2.7234 \times 10^{-3}$	2.11	5	1408	77.812

If we increase the aspect ratio of the ellipse further, we can approximate the situations in which the domain has cracks; see Figure 5, in which we tried to find the



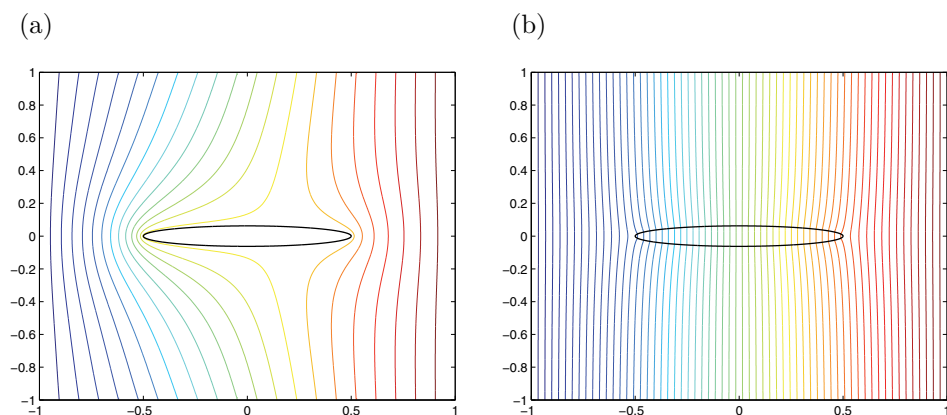


FIG. 5. Electric potential in a domain containing a thin elliptic object. (a) The conductivity of the object is large (1 : 1000). (b) The conductivity of the object is small (1000 : 1).

electric potential in a domain containing an approximated crack  $\varphi(x, y) = (x/0.5)^2 + (y/0.0625)^2 - 1$  within the domain  $[-1, 1] \times [-1, 1]$ . In this case, we have the PDE of  $\nabla \cdot (\beta \nabla u) = 0$ ,  $[u]_\Gamma = 0$ , and  $[\beta u_n]_\Gamma = 0$ , where  $\beta$  is the conductivity. The potential is given at the boundary with high potential on the right. Figure 5(a) is the case with the ratio  $\beta^+ : \beta^- = 1 : 1000$ , while in Figure 5(b) the ratio is  $\beta^+ : \beta^- = 1000 : 1$ . Note that we have tested the code against the analytic solution (6.6) for which we get the same convergence order. More sophisticated techniques and analysis can be found in [17, 64, 56, 52, 63].

In Table 8, we show a grid refinement analysis for the five-star interface  $\varphi(x, y) = r - (0.5 + 0.2 \sin \theta)$  in polar coordinates  $(r, \theta)$ ,  $0 \leq \theta < 2\pi$ . While we still observe average second order convergence for the global solution and the gradient at the interface, the errors are fluctuated more evenly, though the average convergence rate is the same compared with the elliptic interface. We do observe that again for complicated interfaces, we need to resolve the interface for an accurate solution and its gradient.

TABLE 8

A grid refinement analysis for Example 6.3 for a general elliptic interface problem with a five-star interface; see Figure 1.

$N$	$E(u)$	$r$	$E(u_n^-)$	$r$	$E(u_n^+)$	$r$	Iter	$N_b$	CPU(s)
32	$9.7746 \times 10^{-1}$		$2.8683 \times 10^1$		4.7767		11	78	0.03
64	$6.5486 \times 10^{-2}$	3.89	1.9417	3.88	$3.2336 \times 10^{-1}$	3.88	10	154	0.10
128	$1.5688 \times 10^{-2}$	2.06	$6.4504 \times 10^{-1}$	1.58	$1.0623 \times 10^{-1}$	1.60	9	308	0.29
256	$1.8890 \times 10^{-3}$	3.05	$1.6617 \times 10^{-1}$	1.95	$3.6157 \times 10^{-2}$	1.55	9	612	1.07
512	$3.8770 \times 10^{-4}$	2.28	$2.9833 \times 10^{-2}$	2.47	$6.7852 \times 10^{-3}$	2.41	9	1226	19.22

**7. Conclusions.** In this paper, we proposed a new augmented immersed interface method (AIIM) for general elliptic interface problems with variable coefficients that have finite jumps across a general interface and nonhomogeneous jump conditions. Not only the computed solution is second order globally, but also its gradient at the interface from each side of the interface. The method is designed for closed smooth interfaces, not for open-ended interfaces such as cracks. For closed interfaces but with corners, the method still can work with possible large errors near the corners. The convergence of the method has been shown both in one and two dimensions

under appropriate regularity assumptions and a piecewise constant  $\beta(\mathbf{x})$ . For a variable coefficient  $\beta(\mathbf{x})$ , the conclusions are still true if  $h$  is small enough, that is, in the asymptotic sense. Whether this can be improved and why the preconditioning technique works well are two open questions.

**Acknowledgments.** The authors would like to thank Dr. Thomas Beale of Duke University for valuable discussions. We are grateful for the help of Dr. Guanyu Chen, a formal graduate student at North Carolina State University. We would like also to thank the anonymous referees for useful suggestions which helped us to improve the quality of the paper.

# REFERENCES

- [1] J. ALBRIGHT, Y. EPSHTEYN, AND K. R. STEFFEN, *High-order accurate difference potentials methods for parabolic problems*, Appl. Numer. Math., 93 (2015), pp. 87–106.
- [2] J. ALBRIGHT, Y. EPSHTEYN, M. MEDVINSKY, AND Q. XIA, *High-order numerical schemes based on difference potentials for 2D elliptic problems with material interfaces*, Appl. Numer. Math., 111 (2017), pp. 64–91.
- [3] G. AUCHMUTY AND P. KLOUČEK, *Spectral solutions of self-adjoint elliptic problems with immersed interfaces*, Appl. Math. Optim., 64 (2011), pp. 313–338.
- [4] G. AUCHMUTY, *Steklov eigenproblems and the representation of solutions of elliptic boundary value problems*, Numer. Funct. Anal. Optim., 25 (2004), pp. 321–348.
- [5] G. AUCHMUTY, *Spectral characterization of the trace spaces  $H^s(\partial\Omega)$* , SIAM J. Math. Anal., 38 (2006), pp. 894–905, <https://doi.org/10.1137/050626053>.
- [6] G. AUCHMUTY AND P. KLOUČEK, *Generalized harmonic functions and the dewetting of thin films*, Appl. Math. Optim., 55 (2007), pp. 145–161.
- [7] I. BABUŠKA, *The finite element method for elliptic equations with discontinuous coefficients*, Computing, 5 (1970), pp. 207–213.
- [8] J. T. BEALE AND A. T. LAYTON, *On the accuracy of finite difference methods for elliptic problems with interfaces*, Comm. Appl. Math. Comput. Sci., 1 (2006), pp. 91–119.
- [9] J. BRAMBLE AND J. KING, *A finite element method for interface problems in domains with smooth boundaries and interfaces*, Adv. Comput. Math., 6 (1996), pp. 109–138.
- [10] B. CAMP, T. LIN, Y. LIN, AND W. SUN, *Quadratic immersed finite element spaces and their approximation capabilities*, Adv. Comput. Math., 24 (2006), pp. 81–112.
- [11] J. R. CANNON AND M. PRIMICERIO, *A two phase Stefan problem with flux boundary conditions*, Ann. Mat. Pura Appl. (4), 88 (1971), pp. 193–205.
- [12] S. CHEN, B. MERRIMAN, P. SMEREKA, AND S. OSHER, *A fast level set based algorithm for Stefan problems*, J. Comput. Phys., 135 (1997), pp. 8–29.
- [13] Z. CHEN AND J. ZOU, *Finite element methods and their convergence for elliptic and parabolic interface problems*, Numer. Math., 79 (1998), pp. 175–202.
- [14] S. CHOU, D. KWAK, AND K. WEE, *Optimal convergence analysis of an immersed interface finite element method*, Adv. Comput. Math., 33 (2010), pp. 149–168.
- [15] Y. EPSHTEYN AND M. MEDVINSKY, *On the solution of the elliptic interface problems by difference potentials method*, in Spectral and High Order Methods for Partial Differential Equations (ICOSAHOM 2014), Selected Papers from the ICOSAHOM Conference (June 23–27, 2014, Salt Lake City, UT), Lecture Notes in Comput. Sci. Eng. 106, R. M. Kirby, M. Berzins, and J. S. Hesthaven, eds., Springer, Cham, Switzerland, 2015, pp. 197–205.
- [16] Y. EPSHTEYN AND S. PHIPPEN, *High-order difference potentials methods for 1d elliptic type models*, Appl. Numer. Math., 93 (2015), pp. 69–86.
- [17] X. FENG, Z. LI, AND L. WANG, *Analysis and numerical methods for some crack problems*, Int. J. Numer. Anal. Model. Ser. B, 2 (2011), pp. 155–166.
- [18] R. M. FURZELAND, *A comparative study of numerical methods for moving boundary problems*, J. Inst. Math. Appl., 26 (1980), pp. 411–429.
- [19] D. GILBARG AND N. S. TRUDINGER, *Elliptic Partial Differential Equations of Second Order*, Classics in Math., Springer-Verlag, Berlin, 2001. Reprint of the 1998 edition.
- [20] Y. GONG, B. LI, AND Z. LI, *Immersed-interface finite-element methods for elliptic interface problems with nonhomogeneous jump conditions*, SIAM J. Numer. Anal., 46 (2008), pp. 472–495, <https://doi.org/10.1137/060666482>.
- [21] W. HACKBUSCH, *Elliptic Differential Equations: Theory and Numerical Treatment*, Springer-Verlag, Berlin, 1992.

- [22] H. HAN, *The numerical solutions of the interface problems by infinite element methods*, Numer. Math., 39 (1982), pp. 39–50.
- [23] A. HANSBO AND P. HANSBO, *An unfitted finite element method, based on Nitsche's method, for elliptic interface problems*, Comput. Methods Appl. Mech. Engrg., 191 (2002), pp. 5537–5552.
- [24] X. HE, T. LIN, AND Y. LIN, *Approximation capability of a bilinear immersed finite element space*, Numer. Methods Partial Differential Equations, 24 (2008), pp. 1265–1300.
- [25] X. HE, T. LIN, AND Y. LIN, *Immersed finite element methods for elliptic interface problems with non-homogeneous jump conditions*, Int. J. Numer. Anal. Model., 8 (2011), pp. 284–301.
- [26] X. HE, T. LIN, AND Y. LIN, *The convergence of the bilinear and linear immersed finite element solutions to interface problems*, Numer. Methods Partial Differential Equations, 28 (2012), pp. 312–330.
- [27] J. HELLRUNG, L. WANG, E. SIFAKIS, AND J. TERAN, *A second-order virtual node method for elliptic problems with interfaces and irregular domains in three dimensions*, J. Comput. Phys., 231 (2012), pp. 2015–2048.
- [28] S. HOU, Z. LI, L. WANG, AND W. WANG, *A numerical method for solving elasticity equations with sharp-edged interfaces*, Commun. Comput. Phys., 12 (2012), pp. 595–612.
- [29] S. HOU AND X.-D. LIU, *A numerical method for solving variable coefficient elliptic equation with interfaces*, J. Comput. Phys., 202 (2005), pp. 411–445.
- [30] T. HOU, Z. LI, S. OSHER, AND H. ZHAO, *A hybrid method for moving interface problems with application to the Hele-Shaw flow*, J. Comput. Phys., 134 (1997), pp. 236–252.
- [31] T. HOU, X. WU, AND Y. ZHANG, *Removing the cell resonance error in the multiscale finite element method via a Petrov-Galerkin formulation*, Comm. Math. Sci., 2 (2004), pp. 185–205.
- [32] T. Y. HOU, J. S. LOWENGRUB, AND M. J. SHELLEY, *Removing the stiffness from interfacial flows with surface tension*, J. Comput. Phys., 114 (1994), pp. 312–338.
- [33] J. KEVORKIAN, *Partial Differential Equations. Analytical Solution Techniques*, Wadsworth & Brooks/Cole Math. Ser., Wadsworth & Brooks/Cole Advanced Books & Software, Pacific Grove, CA, 1990.
- [34] P. KLOUČEK, D. C. SORESENSEN, AND J. L. WIGHTMAN, *The approximation and computation of a basis of the trace space  $H^{1/2}$* , J. Sci. Comput., 32 (2007), pp. 73–108.
- [35] D. Y. KWAK, K. T. WEE, AND K. S. CHANG, *An analysis of a broken  $P_1$ -nonconforming finite element method for interface problems*, SIAM J. Numer. Anal., 48 (2010), pp. 2117–2134, <https://doi.org/10.1137/080728056>.
- [36] W. J. LAYTON, F. SCHIEWECK, AND I. YOTOV, *Coupling fluid flow with porous media flow*, SIAM J. Numer. Anal., 40 (2003), pp. 2195–2218, <https://doi.org/10.1137/S0036142901392766>.
- [37] R. J. LEVEQUE, *Finite Difference Methods for Ordinary and Partial Differential Equations: Steady-State and Time-Dependent Problems*, SIAM, Philadelphia, 2007, <https://doi.org/10.1137/1.9780898717839>.
- [38] R. J. LEVEQUE AND Z. LI, *The immersed interface method for elliptic equations with discontinuous coefficients and singular sources*, SIAM J. Numer. Anal., 31 (1994), pp. 1019–1044, <https://doi.org/10.1137/0731054>.
- [39] Z. LI, *A fast iterative algorithm for elliptic interface problems*, SIAM J. Numer. Anal., 35 (1998), pp. 230–254, <https://doi.org/10.1137/S0036142995291329>.
- [40] Z. LI, *The immersed interface method using a finite element formulation*, Appl. Numer. Math., 27 (1998), pp. 253–267.
- [41] Z. LI, *On convergence of the immersed boundary method for elliptic interface problems*, Math. Comp., 84 (2015), pp. 1169–1188.
- [42] Z. LI AND K. ITO, *Maximum principle preserving schemes for interface problems with discontinuous coefficients*, SIAM J. Sci. Comput., 23 (2001), pp. 339–361, <https://doi.org/10.1137/S1064827500370160>.
- [43] Z. LI AND K. ITO, *The Immersed Interface Method: Numerical Solutions of PDEs Involving Interfaces and Irregular Domains*, Frontiers Appl. Math. 33, SIAM, Philadelphia, 2006, <https://doi.org/10.1137/1.9780898717464>.
- [44] Z. LI, T. LIN, AND X. WU, *New Cartesian grid methods for interface problem using finite element formulation*, Numer. Math., 96 (2003), pp. 61–98.
- [45] Z. LI AND B. SONI, *Fast and accurate numerical approaches for Stefan problems and crystal growth*, Numer. Heat Transfer B Fund., 35 (1999), pp. 461–484.

- [46] Z. LI, L. XI, Q. CAI, H. ZHAO, AND R. LUO, *A semi-implicit augmented IIM for Navier-Stokes equations with open and traction boundary conditions*, J. Comput. Phys., 297 (2015), pp. 182–193.
- [47] T. LIN, Y. LIN, AND W. SUN, *Error estimation of a class of quadratic immersed finite element methods for elliptic interface problems*, Discrete Contin. Dyn. Syst. Ser. B, 7 (2007), pp. 807–823.
- [48] T. LIN AND X. ZHANG, *Linear and bilinear immersed finite elements for planar elasticity interface problems*, J. Comput. Appl. Math., 236 (2012), pp. 4681–4699.
- [49] T. LIN, Y. LIN, AND X. ZHANG, *Partially penalized immersed finite element methods for elliptic interface problems*, SIAM J. Numer. Anal., 53 (2015), pp. 1121–1144, <https://doi.org/10.1137/130912700>.
- [50] J. LIU, *Open and traction boundary conditions for the incompressible Navier-Stokes equations*, J. Comput. Phys., 228 (2009), pp. 7250–7267.
- [51] X. LIU, R. FEDKIW, AND M. KANG, *A boundary condition capturing method for Poisson's equation on irregular domain*, J. Comput. Phys., 160 (2000), pp. 151–178.
- [52] V. MARTIN, J. JAFFRÉ, AND J. E. ROBERTS, *Modeling fractures and barriers as interfaces for flow in porous media*, SIAM J. Sci. Comput., 26 (2005), pp. 1667–1691, <https://doi.org/10.1137/S1064827503429363>.
- [53] R. MASSJUNG, *An unfitted discontinuous Galerkin method applied to elliptic interface problems*, SIAM J. Numer. Anal., 50 (2012), pp. 3134–3162, <https://doi.org/10.1137/090763093>.
- [54] M. MEDVINSKY, S. TSYNKOV, AND E. TURKEL, *The method of difference potentials for the Helmholtz equation using compact high order schemes*, J. Sci. Comput., 53 (2012), pp. 150–193.
- [55] S. L. MITCHELL AND M. VYNNYCKY, *Finite-difference methods with increased accuracy and correct initialization for one-dimensional Stefan problems*, Appl. Math. Comput., 215 (2009), pp. 1609–1621.
- [56] F. MORALES AND R. E. SHOWALTER, *The narrow fracture approximation by channeled flow*, J. Math. Anal. Appl., 365 (2010), pp. 320–331.
- [57] M. PRUITT, *Large time step maximum norm regularity of L-stable difference methods for parabolic equations*, Numer. Math., 128 (2014), pp. 551–587.
- [58] M. PRUITT, *Maximum norm regularity of periodic elliptic difference operators*, ESAIM Math. Model. Numer. Anal., 49 (2015), pp. 1451–1461.
- [59] V. S. RYABEN'KII, *Method of Difference Potentials and Its Applications*, translated from the 2001 Russian original by N. K. Kulman, Springer Ser. Comput. Math. 30, Springer-Verlag, Berlin, 2002.
- [60] N. SUKUMAR, D. L. CHOPP, AND B. MORAN, *Extended finite element for three-dimensional fatigue crack propagation*, Engng. Fracture Mech., 70 (2003), pp. 29–48.
- [61] L. B. WAHLBIN, *Superconvergence in Galerkin Finite Element Methods*, Lecture Notes in Math. 1605, Springer-Verlag, Berlin, 1995.
- [62] J. WANG AND Y. XIU, *A weak Galerkin finite element method for second-order elliptic problems*, J. Comput. Appl. Math., 241 (2013), pp. 103–115.
- [63] A. WIEGMANN, *Analytic solutions of a multi-interface transmission problem and crack approximation*, Inverse Problems, 16 (2000), pp. 401–411.
- [64] A. WIEGMANN, Z. LI, AND R. LEVEQUE, *Crack jump conditions for elliptic problems*, Appl. Math. Lett., 12 (1999), pp. 81–88.
- [65] H. WU AND Y. XIAO, *An Unfitted hp-Interface Penalty Finite Element Method for Elliptic Interface Problems*, preprint, 2010, <https://arxiv.org/abs/1007.2893>.
- [66] J. XU, *Error estimates of the finite element method for the 2nd order elliptic equations with discontinuous coefficients*, J. Xiangtan Univ., 1 (1982), pp. 1–5.
- [67] X. YANG, B. LI, AND Z. LI, *The immersed interface method for elasticity problems with interface*, Dyn. Contin. Discrete Impulsive Syst., 10 (2003), pp. 783–808.
- [68] W.-J. YING AND C. S. HENRIQUEZ, *A kernel-free boundary integral method for elliptic boundary value problems*, J. Comput. Phys., 227 (2007), pp. 1046–1074.
- [69] Z. ZHANG AND A. NAGA, *A new finite element gradient recovery method: Superconvergence property*, SIAM J. Sci. Comput., 26 (2005), pp. 1192–1213, <https://doi.org/10.1137/S1064827503402837>.
- [70] Y. C. ZHOU, S. ZHAO, M. FEIG, AND G. W. WEI, *High order matched interface and boundary method for elliptic equations with discontinuous coefficients and singular sources*, J. Comput. Phys., 213 (2006), pp. 1–30.